Can seamounts in the Gulf of Alaska be a spawning ground for sablefish settling in coastal nursery grounds?

G.A. Gibson[a,*], W.T. Stockhausen[b], K. Shotwell[b], A.L. Deary[b], J.L. Pirtle[c], K.O. Coyle[d], A.J. Hermann[e,f]

[a]*International Arctic Research Center, University of Alaska, Fairbanks, AK 99775-7340, USA*
[b]*Alaska Fisheries Science Center, NOAA/NMFS, 7600 Sand Point Way, NE, Seattle, WA 98115-6349*
[c]*NMFS Alaska Region, Habitat Conservation Division, P.O. Box 21668 709 W. 9th St., Rm 420, Juneau, AK, 99802-1668*
[d]*Institute of Marine Science, University of Alaska, Fairbanks, AK 99775, USA*
[e]*Joint Institute for the Study of the Atmosphere and Ocean, University of Washington, Seattle WA 98195*
[f]*Pacific Marine Environmental Laboratory, NOAA, Seattle, WA 98115*

Key words: Sablefish, Seamounts, Modelling, Fish larvae, Gulf of Alaska

*Corresponding author. *E-mail address*: gagibson@alaska.edu (G.A. Gibson)

Abstract

In addition to their prevalence on the continental shelf, adult sablefish have been found over the chain of seamounts far offshore in the Gulf of Alaska (GOA). Many of the females that were observed had recently spawned or were ready to spawn. However, to date, it is not known what role the seamounts play in sablefish life history and there are no observations of sablefish eggs or larvae over the GOA seamounts. Due to their depth and remoteness, there are no suitable shallow nursery areas in the vicinity of the seamounts. For successful recruitment, individuals hatching from eggs spawned over seamounts would need to be transported hundreds of miles to suitable areas inshore. Using an individual-based model (IBM) of sablefish, we have demonstrated that if spawning occurs over any of the seamounts in the GOA seamount province it is likely that at least some individuals will be successfully transported to shallow inshore nursery areas in the coastal GOA. As our simulated individuals only exhibit vertical movement behavior this on-shore transport results from the prevailing currents to which they were subjected and not from any geographic or environmental homing capabilities. Our analysis indicates that the strength of the on-shelf velocity is not the primary factor in determining the likelihood of transport to nursery areas. We speculate that the size, strength, location, and direction of the eddies that populate the GOA in any given year could be important in determining transport success. This idea is reinforced by our path analysis which shows that there are markedly different pathways taken by successful individuals among years. Our findings suggest that it may be necessary to expand what is considered suitable habitat for young sablefish. With seamounts being a potentially important spawning site for sablefish, future research priorities should include ground-truthing with fishery or fishery-independent data collected from seamounts. Potential applications of this expanded sablefish IBM include testing for connectivity between seamount and slope spawning areas and the Aleutian Islands and Bering Sea and contributing to the development of spatially explicit assessment models of sablefish.

1. Introduction

Sablefish are a groundfish of high commercial value (Fissel *et al*., 2012; Marquez, 2020) and the majority of the fishery catch is in the Gulf of Alaska (GOA; Hanselman *et al*., 2014), despite their extensive range that spans the west coast of Japan, up to the northern Bering Sea, and as far south as Baja California (Hart, 1973; Sasaki, 1985; Wolotira *et al*., 1993, DFO, 2013; Zolotov *et al*., 2021). Because it is such a lucrative fishery, even small changes to the annual catch results in significant changes to the total value of the catch. Optimized catch quotas that maximize catch while protecting the stock can be informed by knowledge of the spatial dynamics of the stock (Hanselman *et al.*, 2014b). Annual stock assessments are primarily informed by longline surveys for older sablefish that document location, size, and movement via tagging. Knowledge of how environmental processes can influence the survival of younger sablefish, before their recruitment to the fishery, is lacking but could also be very valuable for ecosystem-based management (Shotwell *et al*., 2014).

Adult female sablefish primarily spawn over 100 miles from shore at depths of ~300-800 m near the edges of the continental slope (Mason *et al*., 1983; Moser *et al.*, 1994; Hunter *et al*., 1989). After hatching at depth, the young sablefish larvae migrate to the upper water column and have a peak abundance in the neuston by late spring (Doyle and Mier, 2015). The young sablefish are still in the neuston in late summer (Sigler, 2001), but many have traversed the continental shelf to shallow, near-shore, nursery grounds (Sasaki, 1985, Rutecki and Varosi, 1997). The young fish spend the winter and following summer in coastal bays and inlets (Maloney and Sigler, 2008; Mason *et al*., 1983; Rutecki and Varosi, 1997) before moving into deeper waters. Bracken (l982) re-captured fish tagged in GOA inshore waters far offshore, some as far away as the Bering Sea, demonstrating extensive adult migrations/movement. It has been proposed that sablefish movements in the North Pacific capitalize on the prevailing current directions, with a general westward movement of younger fish, out of the GOA and into the Bering Sea while the larger more mature sablefish return eastwards to the GOA to spawn (Bracken, 1982; Heifetz and Fujioka, 1991; Maloney, 2004). However, other studies found no relationship between sablefish age, size, or sex and movement (Beamish and McFarlane, 1988). More recently it has been shown that adult movement probabilities in the GOA vary annually and can be both westwards (29%) and eastwards (30%; Hanselman *et al.*, 2014b). Sablefish spawning is thought to occur primarily over the shelf break in the central and eastern GOA (Funk and Bracken, 1984; Beamish *et al*. 1983). An individual-based model (IBM) of sablefish indicates that eggs spawned over the continental shelf break in the eastern GOA were much more likely to produce successful settlers than those spawned over the western continental shelf (Gibson *et al*., 2019). This modeling study also suggested that behavioral traits, or physical processes finer than those captured by the model's 3km horizontal resolution, were responsible for the transport of sablefish larvae to some of the better-known nursery areas.

In addition to their prevalence on the continental shelf, adult sablefish have been found over the chain of seamounts far offshore in the GOA (Alton, 1986). These seamounts were formed by volcanic activity and rise from the ocean floor at depths of 3,200–4,000 m to within a few hundred meters of the ocean surface. The GOA Seamount Province (**Figure 1**) comprises nine named seamounts and several smaller ones that range in size from <10 to 70 nmi^2. Approximately half of these seamounts are located within the U.S. exclusive economic zone and are protected as habitat areas of particular concern (Maloney, 2004; NMFS, 2006). The crests on the majority of the seamounts in this chain are relatively flat with a soft substrate (Hughes,

1981). Most of the seamounts in the chain have a crest that is ~649-823 meters below the ocean surface while at 421-549 meters below the surface, the Dickens crest is notably shallower (Hughes, 1981). The crest of the Bowie seamount is shallower still at only 65-100 m below the surface (Herzer, 1971). Tagged sablefish released in the Aleutian Islands, the Bering Sea, and the western and central GOA have been recovered on GOA seamounts (Shaw and Parks, 1997) and sablefish tagged on the GOA seamounts have been re-captured on the GOA continental shelf (Kimura *et al*, 1998; Maloney, 2004). Similarly, tagging evidence suggests migration between the Bowie Seamount and the US west coast (Murie *et al*., 1995; Beamish and Neville, 2003; Whitaker and McFarlane, 1997). In addition to the migration of sablefish to and from the seamounts, retention of adult sablefish over seamounts can also occur (Maloney, 2004). Maloney (2004) suggested that the use of the GOA seamounts is part of the general migratory circulation pattern that roughly follows the prevailing currents as the adult sablefish move back towards the eastern GOA. However, the ability of sablefish to exert such highly migratory behavior could allow suitable seamount habitat to be exploited independent of currents (Hoff and Stevens, 2005).

The sablefish found over the GOA seamounts span many year classes (55 for males and 33 for females; Maloney, 2004), suggesting that the use of the seamounts is a common part of sablefish life history. As has been noted in other sablefish populations (Kapur *et al*., 2021), the sex-ratio of the seamount population is skewed toward males, with a ratio of at least a 2:1 occurrence of males to females (Hughes, 1981; Maloney, 2004). With an average age ranging from 13.7-30 years, the males are generally older than the females (9.8-23.8 years) but the females tend to be larger (Maloney, 2004). Many of the females that were observed over the GOA seamounts had recently spawned or were ready to spawn but, to date, there are no observations of young sablefish in the vicinity. However, sampling has been sparse, with sablefish initially observed during an exploration of the USA seamounts in 1979 (Hughes, 1981) and then again during targeted sampling in 1999-2002 (Maloney, 2004). In both cases, sampling occurred during the summer (June or July) and used longline fishing gear which would miss smaller individuals in the upper water column. It is also possible that young sablefish were missed due to a mismatch in the timing of sampling.

The presence of spawning-capable sablefish suggests that spawning might occur over seamounts; however, due to their depth and remoteness, there are no suitable shallow nursery areas in the vicinity of the seamounts. For successful recruitment, individuals hatching from eggs spawned over seamounts would need to be transported to suitable areas inshore, a distance of at least 270 miles. Understanding the potential of the GOA seamounts to support sablefish spawning and recruitment to the fishery would provide a more complete picture of sablefish life history. If seamounts are viable spawning sites, interannual variation in larval transport from these locations could explain some of the variability in annual recruitment success. The importance of such secondary spawning sites may increase as ocean conditions change, altering development rates and transport pathways.

Due to limited empirical data on sablefish distributions near seamounts, IBMs, that pair species-specific biological characteristics of early life stages with modeled ocean currents and conditions, are useful tools for exploring potential connectivity between spawning and nursery sites (Gibson *et al*., 2019, Stockhausen *et al.*, 2019, Hinckley *et al*., 2019). Each life stage in

Gibson *et al*.'s (2019) sablefish IBM was assigned specific depth preferences and vertical swimming speeds. The transition between each life stage depends on the individual size. As size is so critical in determining life stage, and thus the depth and current regime that an individual is exposed to, it is important to represent larval growth rates as realistically as possible. Here, we update the original sablefish IBM (Gibson *et al*., 2019) to include stage-specific temperature-dependent growth rates, and then use this model to address the hypotheses that 1) sablefish spawned over the GOA Seamount Province can be successfully transported to the inshore nursery area regions and 2) some seamounts are more likely than others to support successful transport to nursery habitats along the coast.

2. Methods

2.1. Model Description

Sablefish dynamics were simulated using a Lagrangian particle tracking IBM coupled to an Eulerian hydrodynamic model of the region. This coupled model set-up has been previously described (Gibson *et al.*, 2019) but, in brief, early life history characteristics (e.g. spawning locations, larval behavior, and growth rates of young sablefish) are simulated using the Dispersal Model for Early Life Stages (DisMELS; Cooper *et al*., 2013, Stockhausen *et al*., 2019). A Regional Ocean Modeling System (ROMS) coupled to a lower trophic level Nutrient-Phytoplankton-Zooplankton (NPZ) model was used to simulate the physical and lower trophic level environment in the GOA through which the simulated sablefish individuals were transported (Coyle *et al*., 2019). The IBM was run for twenty-two consecutive years, from 1997 to 2018.

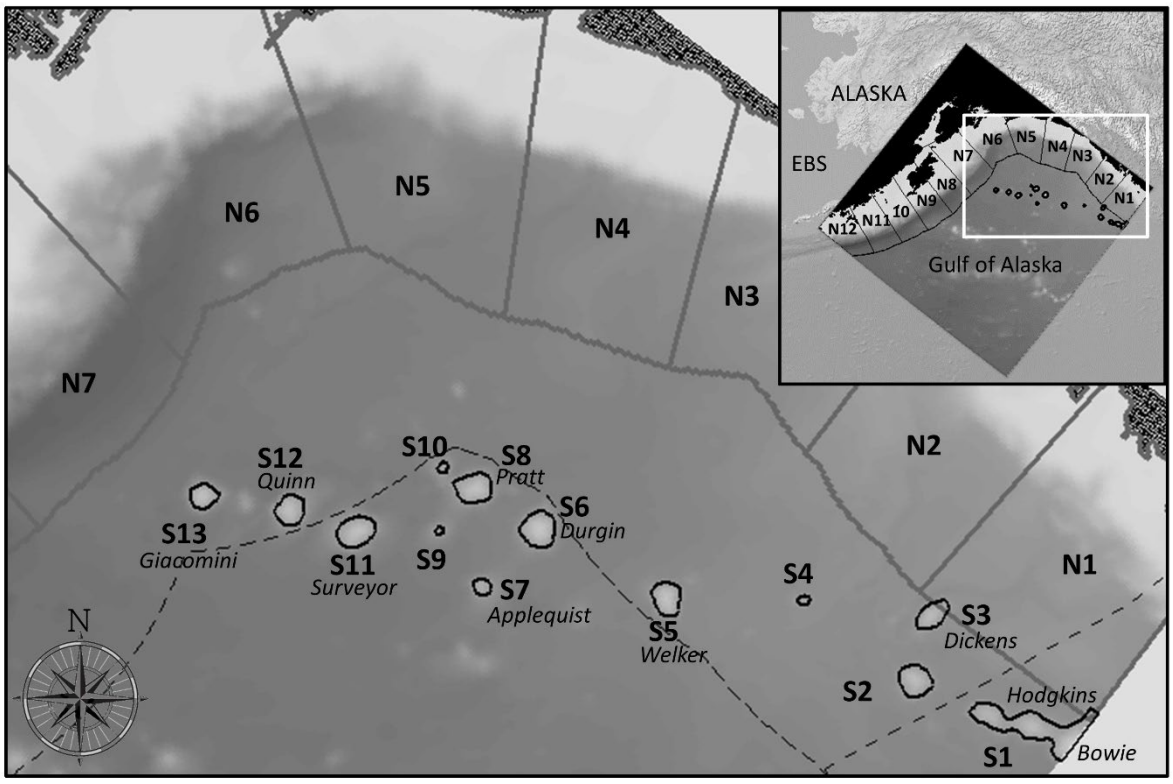

Figure 1. Location of the thirteen seamounts (S1-S13) in the Gulf of Alaska seamount province and the twelve alongshore regions (N1-N12) used in our connectivity analysis. The location of the US Exclusive economic zone as provided by Flanders Marine Institute (2019) is also shown (dashed line).

2.2. Physical model

The GOA ROMS-NPZ skill in resolving common physical and biological features in the GOA has been previously documented (Hinckley *et al.*, 2009; Dobbins *et al.*, 2009; Cheng *et al*., 2012; Coyle *et al*., 2013; Hermann *et al*., 2009; 2016). These models have been used to drive other IBMs (Stockhausen *et al*., 2019; Hinckley *et al.*, 2019), including the predecessor to the sablefish IBM (Gibson *et al*., 2019) presented here. Here we use a slightly updated version of the NPZ model, as described in Coyle *et al*. (2019). The ROMS GOA model has a horizontal resolution of approximately 3 km with ~500 × 500 grid points. Grid boundaries extend from the Shumagin Islands (162.74°W) in the western GOA to Prince of Wales Island in the eastern Gulf (132.10°W), and from 46.66°N in the GOA basin up through Prince William Sound (64.19°N, **Figure 1**). The model has 42 vertical layers and uses a stretched z-coordinate system that allows vertical refinement to resolve the surface boundary layer. The thickness of the upper layer follows the bathymetry and varies from ~0.5 m over the shallow continental shelf to ~5-10 m over the deeper ocean basin. The ROMS GOA model uses bathymetry based on ETOPO5 and supplementary data as described in Danielson *et al*. (2016); smoothing of bathymetry was applied for numerical stability. Any oceanic regions shallower than 10 m were set to 10 m deep. Daily averages for physical oceanographic fields from the ROMS model were low-pass filtered to eliminate tidal aliasing and were used to drive the IBM simulations within the DisMELS framework. Since the development of the original Sablefish IBM (Gibson *et al*., 2019) the physical model was updated to use an improved representation of freshwater discharge along the coastline. The new configuration is based on the fine-scale coupled land hydrology models of Beamer *et al*. (2016) and has higher and deeper seasonal peaks and valleys that the original runoff model (Royer *et al*., 1982) due to increased spatial and temporal resolution (Hill *et al*., 2015) as described in Coyle *et al*. (2019). Significant differences between these two products have been discussed in Danielson *et al*. (2020); these include a climatological peak runoff in July using the newer method, as compared to October from the older method.

2.3. IBM model

The sablefish IBM simulates five life stages including fertilized eggs, yolk-sac larvae, feeding larvae, epi-pelagic juveniles, and 'settled' juveniles (**Figure 2**). Parameter selections and sources for most parameters remain the same as the original model (Gibson *et al*., 2019) but while the original model had stage-specific constant growth rates, here we have updated the model to include temperature-dependent growth rates and behaviors. The growth rate equations are described below, while the stage-specific parameters i.e. depth preference, vertical swimming speed, minimum and maximum stage duration, and transition size retain their original values (Gibson *et al*., 2019, cf. Table 1) unless otherwise noted. A detailed parameter sensitivity analysis found results to be relatively robust to parameter values (Gibson *et al*., 2019). As in the previous version, individuals are presumed unable to exhibit complex horizontal movement behavior strong enough to overcome horizontal currents, thus their position is determined

through advection from the ROMS model. However, individuals can control their vertical position in the water column according to their stage-specific "preferred" depth range and a mean vertical swimming speed. Space is considered to be continuous for the individuals i.e., they can move around, and their location is tracked within the ROMS grid cells. To ensure that the advection and biological processes of each individual were adequately resolved, the sablefish IBM used a sub-daily integration time-step of twenty minutes. At each of these biological time steps, the three-dimensional currents and temperature and NPZ fields from the daily ROMS-NPZ model output were interpolated to each individual's location.

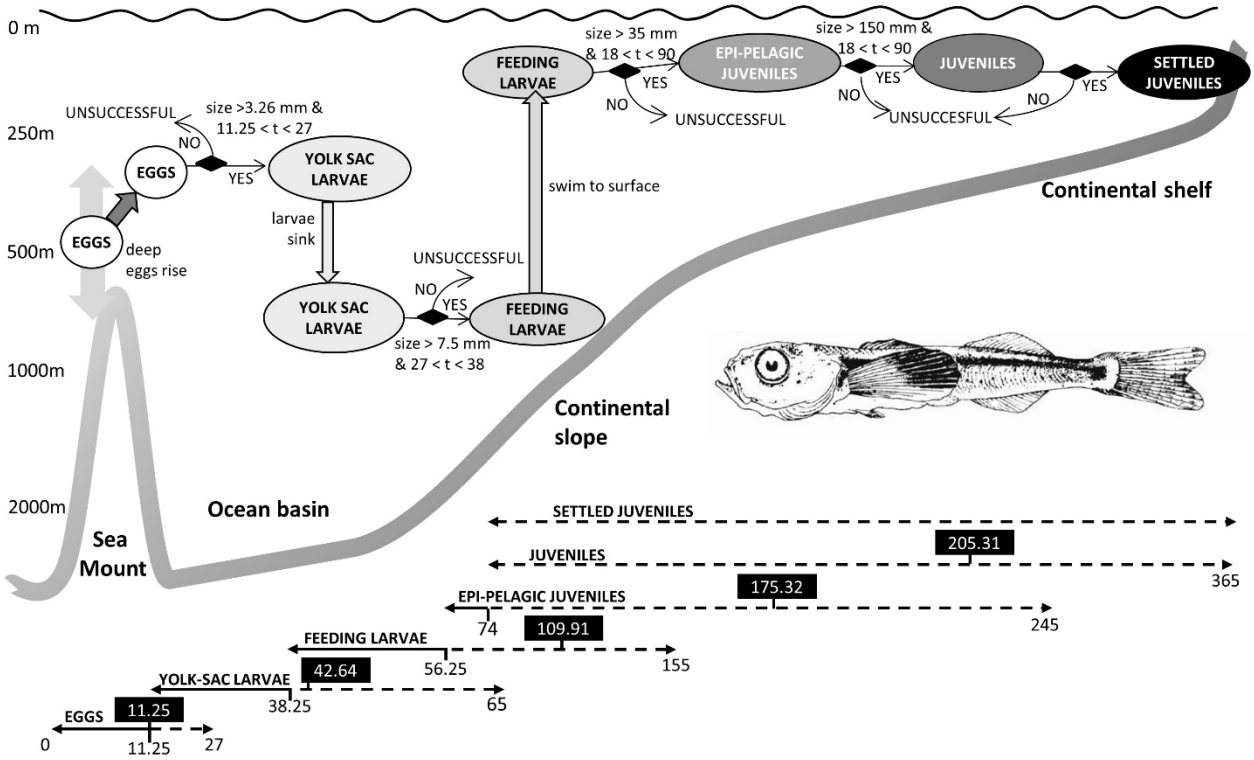

Figure 2. Conceptual view (not to scale) of the sablefish individual-based-model, illustrating the life stages, assumed depth preferences, and rules determining progression from one life stage to the next. Movement from offshore spawning sites to inshore nursery sites is passive and dependent on advection. The inset figure shows a late-stage sablefish larvae (SL 33 mm) reproduced from Kendall and Matarese (1987). Black diamonds represent stage transition and associated rules for transition. See text and Gibson *et al*. (2019, cf. Table 1) for a description of model parameters. The potential time-period (days from initialization) that individuals could spend in each life stage is indicated, along with the mean transition time (white text on black) simulated for individuals from all seamounts and years.

2.3.1. Egg stage

Individual 'sablefish' particles were initialized over the seamounts at the egg stage. All eggs were assumed fertile, with the ability to develop to the hatching stage. To reflect current understanding of vertical positioning of eggs in the water column (Alderdice *et al*., 1988) eggs are assumed capable of adjusting their vertical position to maintain a depth between 213 and

360 m. In reality, egg size is related to maternal factors (i.e. female size, female age, female condition, batch number, etc.). To encapsulate some of this variability, in our updated version of the model, egg size (S_{egg}) at spawning is randomly assigned from a uniform distribution within the observed size range (1.8 and 2.2 mm, Mason *et al*., 1983). While the simulated eggs do not technically grow in size, the time that the larvae take to hatch, and their size at hatch does vary. The number of days until hatch (DTH, **Eq. 1**) was simulated using a temperature-dependent quadratic formula fitted to observational data (Alderice *et al*., 1988, Jensen and Damon 2002, Deary *et al.*, 2019, **Figure 3a**).

$$DTH = 0.4046 \cdot T^2 - 6.307 \cdot T + 35.53, \quad \text{where } 11<\text{DTH}<27 \tag{1}$$

Using the few available data points (Alderice *et al*., 1988; Deary *et al*., 2019) we approximated the size of larvae at hatch (S_H, **Eq. 2**) to be a linear temperature-dependent function (**Figure 3b**).

$$S_H = -0.4189 \cdot T + 6.702 \tag{2}$$

From **Eq. 1** and **Eq. 2**, we approximated a growth rate for the embryos (GR_{egg}, $\boldsymbol{Eq.3}$) by assuming an average initial egg size of 2mm.

$$GR_{egg} = \frac{S_H - 2}{DTH}, \quad GR_{egg} \geq 0 \tag{3}$$

This gave growth rates that varied between 0 and 0.18 mm/day for temperatures from -2 to 11.2°C with a maximum at 5°C (**Figure 3c**). Temperatures exceeding 11.2°C would result in negative growth rates, so we assumed that growth does not occur in waters warmer than 11.2°C and set the associated growth rate to zero. The minimum time required for eggs to develop and hatch into yolk-sac larvae is 11.25 days, and a size of 3.26 mm had to be reached before an egg was considered hatched. Embryos that failed to reach the minimum size required for the transition to the next life stage within the allotted timeframe (twenty-seven days) were considered unsuccessful. Within this series of experiments, we found that all individuals reached transition size by 11.25 days and made the transition to yolk-sac larvae at that time.

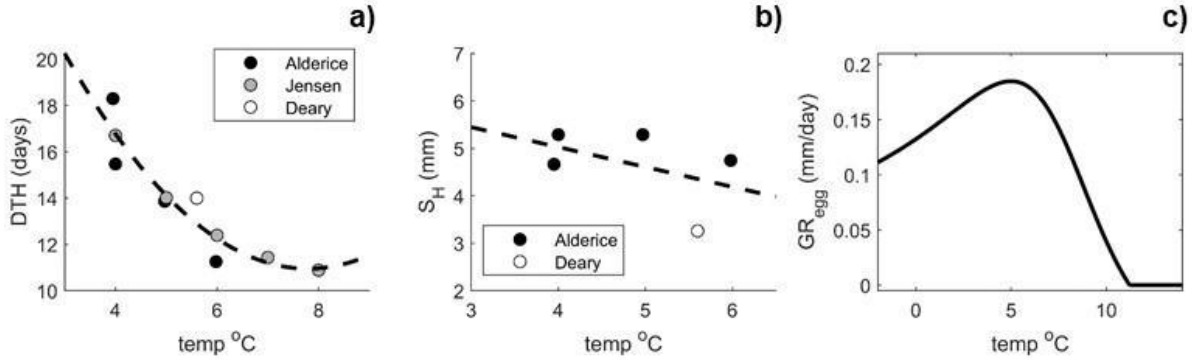

Figure 3. Data and formulations used to simulate egg growth rate. a) Days until hatch (DTH) vs. temperature. Observational data is from Alderice *et al.*, 1988 (black), Jensen and Damon 2002 (grey), and Deary *et al.*, 2019 (white). Data was fitted with the quadratic curve $DTH = 0.4 \cdot T^2 - 6.3 \cdot T + 35.5$, R^2=0.89. b) Size (S_H) of larvae at hatch is estimated to be a temperature-dependent linear function of temperature with data Alderice *et al.*, 1988 (black) and Deary *et*

al., 2019 (white) and function $S_H = -0.4189 \cdot T + 6.702$, R^2=0.21. c) Estimated temperature-dependent growth rate for sablefish embryos using the formulation presented in **Eq. 3**.

2.3.2. Yolk-sac larval stage

Observational data (Alderice *et al.* 1988; Deary *et al*., 2019) indicates that yolk sac larvae (YSL) size increases linearly with days post-hatch (DPH, **Figure 4**) with the relationship shown in **Eq. 4**.

$$S_{YSL} = 0.1105 \cdot DPH + 4.624 \quad (4)$$

The slope of the line (0.11 mm/day) is the temperature-independent growth rate we assumed for YSL. Following a minimum of 27 days at this stage, the point at which feeding apparatus could have developed and feeding might occur (Deary *et al*., 2019), the larvae were assumed to have used up their yolk sac and transitioned to the feeding larvae life stage, provided they reached a minimum size of 7.5 mm. Individuals that did not reach the required size prior to 38 DPH were considered unsuccessful. YSL have been observed to exhibit mass mortality (50%) when temperatures exceed 9°C (Deary, per. Comm.). Thus, we assumed that temperatures higher than this were lethal for this life stage. Within this series of experiments, we found the mean age of transition to feeding larvae to be 42.64 days from spawning.

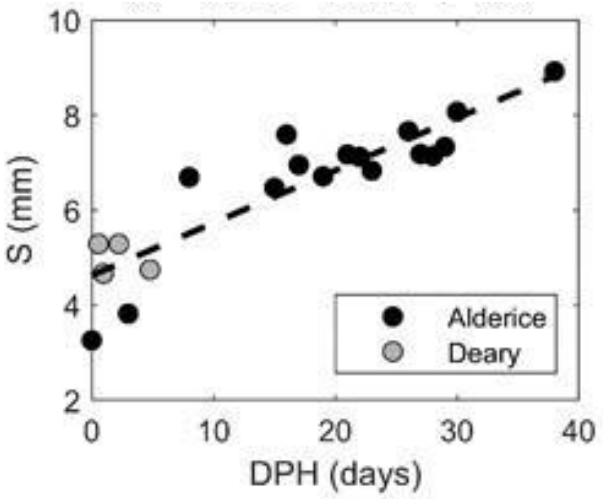

Figure 4. Data and formulations used to simulate yolk sac larvae size as a function of the number of days post-hatch (DPH). Data from Alderice *et al*., 1988 (black) and Deary *et al*., 2019 (grey). Data were fitted with the linear equation $S = 0.11 \cdot DPH + 4.6$, R^2=0.82. The slope of the line, representative of the constant daily growth rate, was 0.11mm/day.

We also assumed that, while yolk-sac larvae can regulate density to maintain their vertical position in the water column after sinking to a depth of 500-1000 m, this stage does not actively swim—reflecting the fact that in the laboratory, newly hatched larvae did not exhibit spontaneous movement (Alderdice *et al*., 1988). Minimum and maximum depths and swim speeds were left unchanged from the previous version of the model.

2.3.3. Feeding larval stage

For the feeding larval stage, we initially fit a quadratic function to the temperature-dependent, length-specific growth rates (SGR, **Eq. 5**) determined by Cook *et al*., (2017) but assumed that the SGR had a minimum of 2.26 %/day, as this was the minimum of the quadratic function which was observed at a temperature of 7.82°C (**Figure 5**).

$$SGR = max(2.26, 0.01556 \cdot T^2 - 0.24 \cdot T + 3.2) \quad (5)$$

Where 2.26 ≤ SGR

While based on only limited growth rate data, this function gives a growth rate that ranges from 0.16mm/day for the smallest individuals in this life stage (7.12mm) at temperatures below 7.82°C, and 1.35mm/day for the largest individuals (35mm) at 18°C. This range encapsulates the constant growth rate parameter (0.48mm/day) that was previously estimated from observations in the original model (Gibson *et al*., 2019).

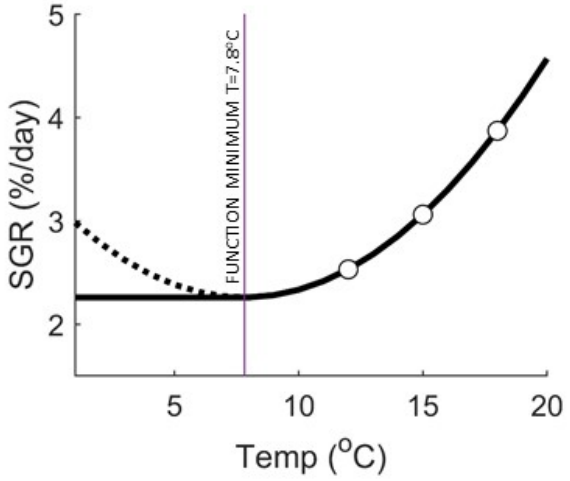

Figure 5. Data and formulations used to simulate feeding larvae specific growth rate (percentage of standard length per day) as a function of temperature. Data came from Cook *et al.*, 2017 (white circles). Data were fitted with the quadratic equation $SGR = 0.01556 \cdot T^2 - 0.24 \cdot T + 3.21$ (R^2=1.0) but growth rates at temperatures below 7.82°C, the temperature at the function minimum, were fixed to 2.26% rather than increasing.

As in the original model, we assumed that following the transition to the feeding larval stage, individuals ascend rapidly in the water column until they reach the surface ocean and actively maintain their position during this life stage. While there is no marked morphological change between the larval and juvenile stages (Kendall and Matarese, 1987), larvae are considered '*epi-pelagic juveniles'* once they have reached a total length of 35 mm. Feeding larvae that fail to reach this size within 90 days are considered unsuccessful. Within this series of experiments, we found the mean age of transition to epi-pelagic juvenilles to be 109.91 days from spawning.

2.3.4. Epi-pelagic juvenile stage

Epi-pelagic juveniles continue to maintain their position in the neuston but grow at a much faster rate than feeding larvae. Following the growth model presented in Boehlert and Yoklavich (1985), the size of individuals in this life stage was assumed to be a function of age (**Eq. 6**, **Figure 6a**). By computing the gradient of this sigmoidal curve, the growth rate as a function of age ($GR_{epi\,A}$) was obtained, which we fit with a cubic equation (**Eq. 7**, **Figure 6b**) for individuals from 48 to 137 days - the minimum and maximum time that an individual could be in the epipelagic juvenile stage. Boehlert and Yoklavich (1985) found the mean growth rate to be 1.47 mm/day. No temperature measurements were reported, but assuming the linear temperature-dependent growth equation fitted to Sogard and Olla (2001) data (**Eq. 8**, **Figure 6c**) we assumed it occurred at a baseline temperature (T_B) of 12.1676°C. Thus, we derived an expression for the temperature and age-dependent growth rate of epi-pelagic juveniles (**Eq. 9**). Observed growth rates at 24°C were markedly reduced (Sogard and Olla, 2001), thus at temperatures ≥23°C, epi-pelagic juvenile growth rate was assumed to drop to 0.345mm/day.

$$Length(Age_{DPH}) = 1.2203 \cdot exp\left(\left(\frac{0.1084}{0.0196}\right) \cdot (1 - exp(-0.0196 \cdot Age_{DPH}))\right) \quad (6)$$

$$GR_{epi\,A} = 2.261 \cdot 10^{-6} {Age_{DPH}}^3 - 0.0009735 \cdot {Age_{DPH}}^2 + 0.1183 \cdot Age_{DPH} - 2.2 \quad (7)$$

$$GR_{epi\,T} = 0.09965 \cdot T + 0.2575 \quad (8)$$

$$GR_{epi} = GR_{epi\,A} + (T - 12.1676) \cdot 0\,.09965 \quad (9)$$

$GR_{epi\,A}$ has a maximum of 2.2198 mm/day at 87 days and 12.1676°C, which increases to a maximum of 3.1996 at 22°C.

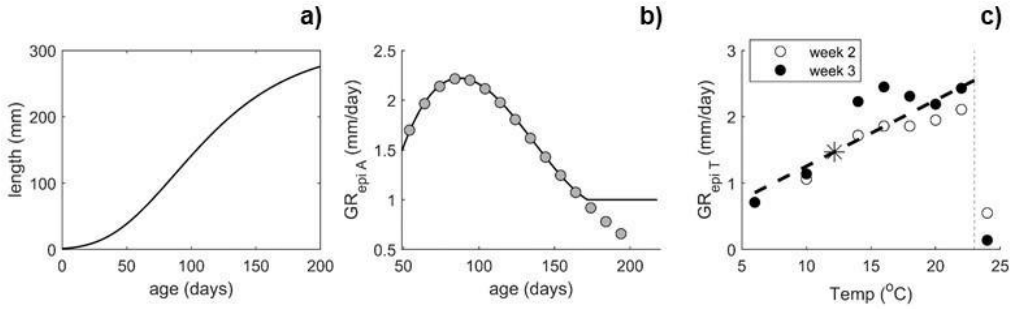

Figure 6. Data and formulations used to simulate epipelagic juvenile growth rate. a) Individuals length vs. age as specified by the Boehlert and Yoklavich (1985) growth equation. b) Age-dependent growth rate determined from the slope of the curve in a) and fitted with the polynomial (**Eq. 7**, R^2=0.999). c) Temperature-dependent growth rates determined by Sogard and Olla (2001). Data are fitted with **Eq. 8**, R^2=0.77). The asterisks indicate the mean growth rate (1.47mm/day) found by Boehlert and Yoklavich (1985), which, following **Eq. 8**, can be assumed to coincide with a temperature of 12.1676°C. The observed growth rates at 24°C were ignored when determining the linear relationship. The growth rate at or above 23°C was assumed to be 0.345 mm/day, the average of the week 2 and week 3 growth rates at 24°C.

Once epi-pelagic juveniles reach 150 mm they are considered *'Juveniles'* with the ability to 'settle' in defined nursery areas, effectively recruiting to the population that will grow and eventually enter the fishery. Within this series of experiments, we found the mean age of transition to juveniles to be 175.32 days from spawning.

2.3.5. Juvenile stage

Following the transition to the juvenile stage, individuals continue to inhabit the upper water column but undertake diel vertical migrations, moving higher in the water column at night (Courtney and Rutecki, 2011; Sogard and Olla, 1998). The growth rate of individuals at this stage is simulated using the temperature-dependent growth rate found for young of the year (YOY) sablefish (Krieger *et al*., 2019, Table 1). We fitted the data with a third-order polynomial (**Figure 7**). Examining the roots of the polynomial, the growth rate was set to a minimum of 0.38 mm/day at temperatures below 3.45°C, and to an overall minimum of 0.0 mm/day to prevent negative growth rates at temperatures exceeding 22.41°C. Maximum growth rate for this stage was 1.34 mm/day at 15.6°C.

As discussed previously (Gibson *et al.,* 2019), juvenile sablefish do not fully transition from the pelagic environment to the benthic environment but they do actively maintain their position over desirable habitats, including inshore bays. Settled early juvenile sablefish habitat in the GOA was previously modeled as the predicted probability of suitable habitat from a presence-only maximum entropy species distribution model (SDM) fitted to their distribution in mixed gear-type surveys and to a suite of environmental covariates (Pirtle *et al*., 2019, Shotwell *et al*., 2022) (**Figure 8**). Here we consider the transition to a "settled" individual to occur if individuals are over depths shallower than 100 m and over locations where the predicted probability of suitable habitat (HSI) is ≥0.4 based on a threshold of equal training sensitivity and specificity from the SDM. When juveniles find themselves over suitable habitat they transition to 'settled juveniles,' and transport to a nursery area is deemed successful. Juveniles that fail to reach a suitable nursery habitat prior to 365 days since initialization (the end of the simulation) are considered unsuccessful. Within this series of experiments, we found the mean age of transition to settled juveniles to be 205.31 days from spawning.

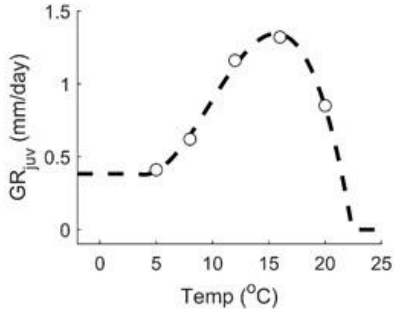

Figure 7. Fitted polynomial used to simulate juvenile sablefish growth rate. Open circles are observed growth rates from Krieger *et al*., 2019

2.3.6. Settled Juvenile stage

Here settled juveniles are considered to have the same growth rate function as juveniles. Settled juveniles for the purpose of this experiment are fixed in both horizontal and vertical position (bottom depth) and the environmental experiences of the individuals are tracked for the remainder of the year since spawned, for a total of 365 days.

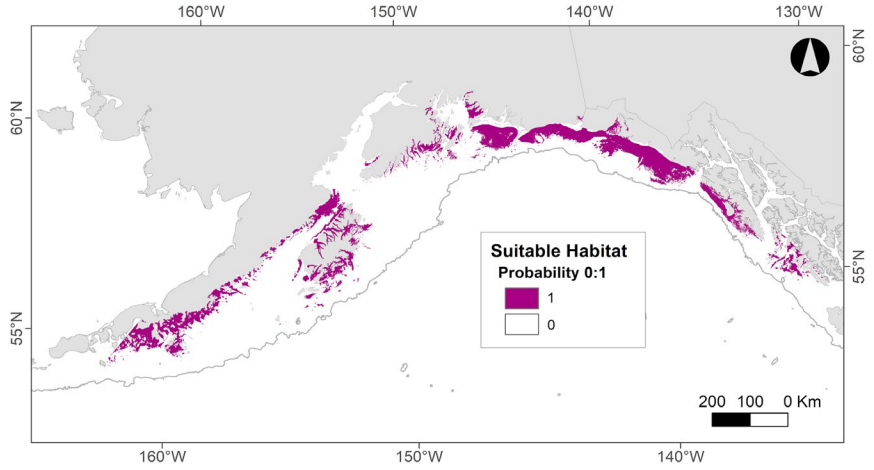

Figure 8: Settled early juvenile sablefish suitable habitat locations in the GOA (shaded areas) inshore of the 1000 m depth contour within the GOA ROMS grid.

2.4. Connectivity Experiment

Seamounts in the Gulf of Alaska were identified by extracting the locations of the 2500m isobath east of 147°W between 53-57°N. A series of thirteen individual polygons were identified that corresponded to both named and unnamed seamounts (**Figure 1**). For each year of the simulation, eggs were released on Feb. 20th, corresponding to the day of peak occurrence of sablefish eggs in the GOA (Doyle and Mier, 2015). Eggs were initialized on a 500m resolution horizontal grid over each of the 13 seamounts at 50 m depth intervals between 300 and 800 meters. A sensitivity analysis of the model output to the horizontal resolution of egg initialization (Gibson *et al*., 2019) previously found that the probability of individuals settling in any nursery area was broadly similar, regardless of their initial spacing (from 500m -25km). Here we opted to use the finer resolution to ensure that smaller-scale dynamics associated with the seamounts were not missed. The size of the seamounts, and thus the number of individuals released over each seamount, varied (**Table 1**), ranging from 846 for S9 to 44,905 for S1 (the Hodkins/Bowie complex), for a total of 161,380 individuals per one-year model iteration.

2.5. Analysis

To assess interannual variability in the transport of young sablefish from potential deep ocean seamount spawning sites to near-shore nursery areas, we calculate the probability of transport from a spawning area to a settlement area for each year. To compare interannual differences in connectivity, we looked at "total connectivity" (the probability of settlement integrated across all spawning areas) and connectivity to/from specific alongshore areas.

2.5.1. Connectivity Analysis

It is not currently known whether sablefish spawn over the seamounts. Therefore, we made the simple assumption that the sablefish spawning stock is uniformly distributed across all seamounts in the Gulf of Alaska Seamount province. This assumption allows us to focus on evaluating the potential *relative* strength of connectivity from each seamount to potential nursery regions. Nursery areas were assumed to be relatively large scale and we divided the entire GOA into twelve approximately equal alongshore zones (**Figure 1**). The locations of individuals were assessed at the end of the model run to determine within which, if any, of the alongshore zones they settled. Settlement only occurred if the depth and habitat suitability criteria were met (see Section 2.3.5). For each model year (y), the strength of connectivity ($C_{N,S}$) between each seamount spawning site and each alongshore settlement site was calculated as the proportion of individuals released over a seamount (S) that settled into a nursery area (N). Annual connectivity matrices $C_{N,S}\ (y)$ were constructed for each year.

$$C_{N,S}\ (y)\ =\ \frac{No.Individuals\ settling\ in\ nursery\ area\ N}{No.Individuals\ spawned\ over\ seamount\ S} \tag{10}$$

The annual connectivity matrices reflect the fraction of individuals released in each spawning area that were successfully "recruited" to each nursery area—independent of the size of the spawning stock in any spawning area. To provide a measure of central tendency, the overall median connectivity for each cell in the matrix was computed from the annual connectivity matrices:

$$M_{N,S} = median\left(C_{N,S}(y)\right)_{y=1997}^{2018} \tag{11}$$

In addition, the overall temporal variability in connectivity was estimated using the temporal median absolute deviation (Leys *et al.*, 2013) of the annual connectivity matrices:

$$\sigma MAD_{N,S} = median_{N,S}\left(abs\left(C_{N,S}(y) - M_{N,S}\right)\right) \cdot 1.4826 \tag{12}$$

To explore the interannual variability in connectivity between spawning and nursery sites, we examined: 1) interannual variability in "total connectivity" (C_{TOT}), the sum of all probabilities in the connectivity matrix for each year.

$$C_{TOT}(y) = \sum_{1997}^{2018} C_{N,S}(y) \tag{13}$$

To examine the covariance structure of connectivity between seamount spawning sites and inshore nursery areas in the GOA in space and time, we employed multivariate empirical orthogonal function (EOF) analysis. The EOF method, outlined in detail in Gibson *et al.*, 2019, derives spatial covariance across the series of annual mean connectivity matrices for each of the twenty-two years simulated. The analysis describes the data in terms of the EOF eigen-modes, ordered by the percentage of the total variance explained by each of the modes, which are statistically uncorrelated with one another. We present the spatial patterns ("modes") and associated Principal Component (PC) time series for the first two modes of the analysis.

2.5.2. *Transport Analysis*

A "Path Analysis" was performed to search for common trajectories or areas of the GOA used heavily by the young sablefish as they are transported away from the seamounts. This was achieved by first binning all trajectory locations for all individuals simulated on all days of the simulation into grid cells, then counting the number of individuals within each grid cell. It is important to note that this bin count can include the same individuals on successive days due to retention within a bin, as well as multiple individuals briefly moving through a bin. For brevity, we present the results for individuals 'spawned' over S5 (the Welker Seamount), the seamount that had the highest fraction of successfully settling individuals, as well as S1 at the eastern end of the chain and S13 at the western end (refer to Figure 1 for seamount locations). We examine 2002, 2007, 2009,2010,2013, and 2018; years indicated by an EOF analysis to have different connectivity patterns.

$$CellCount_{eta,xi} = \sum_{1}^{365} No.\,individuals\ in\ cell_{eta,xi} \tag{14}$$

2.5.3. *Environmental Indices*

We explored the correlation between a collection of environmental indices and the 1st principle component (PC1) from our EOF analysis. Temperature and transport are thought to impact sablefish recruitment (Shotwell *et al*., 2014; Gibson *et al*., 2019) and thus were the focus of our environmental analysis in addition to the Arctic Oscillation index, a large-scale climate index that impacts the North Pacific. Specific indices considered included the temperature along the upper 100m of the 500m isobath, the across-shelf and along-shelf velocity, and the Arctic Oscillation index (AO). To compute the along-shelf and across-shelf flow we first extracted the latitude and longitude of the 500m isobath from the ROMS model grid. Modeled u and v velocity components in the upper 100m were interpolated to these locations along the 500m isobath. Examples of the spatially explicitly annual averaged velocity over the GOA, along with the location of the 500m isobath, are shown in Appendix A for 2010 and 2018. From the gradient of the isobath location, we then resolved the velocities into along-shelf and across-shelf components of velocity. The monthly climatology of temperature, salinity, and velocity at each spatial point was determined and this seasonal cycle was removed from the time-series. Finally, the oceanographic variables were averaged seasonal (JFM, AMJ, JAS, OND) and annual over 5-degree bins to give indices for the eastern (135-140°W), east-central (140-145 °W), west-central (145-150 °W), and western (150-155°W) Gulf.

The AO (Thompson and Wallace, 1998) provides a measure of the atmospheric circulation over the Arctic. It consists of a positive phase when surface pressure in the polar region is below average and low and the cold Arctic air (polar vortex) is restricted to the polar region and a negative phase where the opposite is true. This atmospheric phenomenon can govern weather and climate patterns across mid- and high-latitude areas. Monthly average data is readily available (https://www.daculaweather.com/4_ao_index.php) and was used to develop annual and seasonally averaged AO indices.

3. Results

Our model experiments indicate that sablefish spawned over any of the seamounts in the Gulf of

Alaska seamount province have the potential to be successfully transported to shallow inshore nursery areas in the coastal Gulf of Alaska; spawning over some seamounts is significantly more likely to produce successful inshore settlement than others. The median connectivity (probability of settlement) from the seamounts to the inshore nursery areas (**Figure 9a**) indicates that eggs spawned over most seamounts are likely to settle in alongshore areas in the central Gulf, primarily in alongshore area 6, followed by alongshore area 7 to the west for eggs originating from seamounts 5-10. The easternmost seamounts were also most strongly connected to area 6, but individuals from these seamounts were secondarily more likely to settle in areas to the east (alongshore areas 4 and 5). Eggs from seamounts S12-S13 have a relatively low probability (<0.1) of settling in any of the alongshore areas. None of the seamounts produced settlers in the easternmost alongshore area (N1). Over the twenty-two-year period examined, the maximum connectivity between an individual spawning area and an individual nursery area was 0.54. This maximum connection was from seamount M9 to nursery area 6 in the central Gulf of Alaska in 2018. The second strongest connection (0.47 in 1997) also occurred between this seamount-nursery area pair. The strongest annual median connectivity (0.23) was between M2 and nursery area N6.

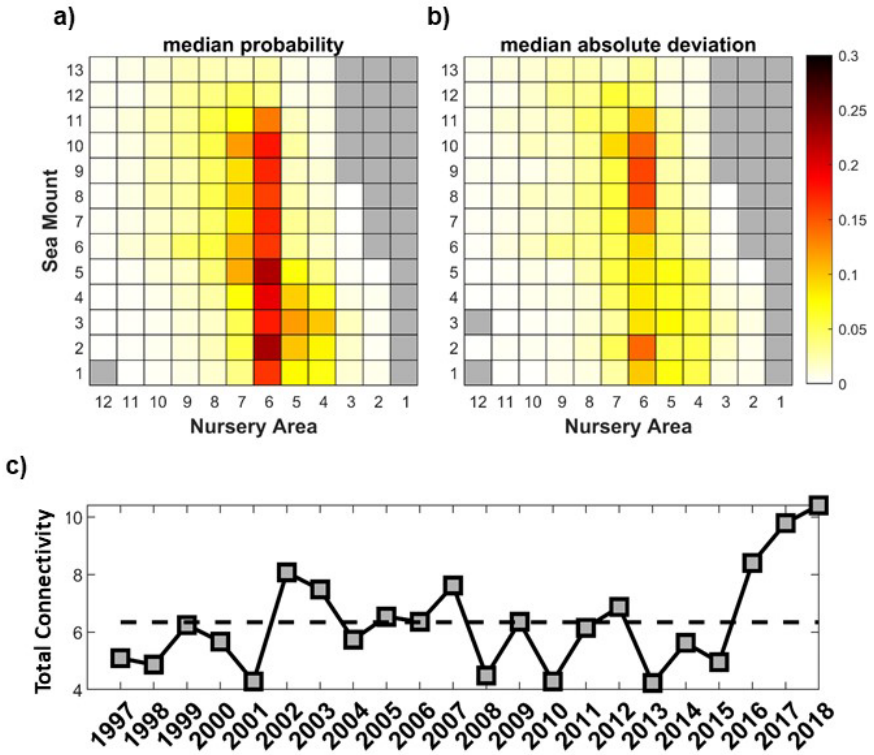

Figure 9. Connectivity matrix showing the median probability that individuals released as eggs over each of the seamount spawning areas successfully settled in each alongshore nursery area (a), the associated deviation about the median (b), and the total connectivity in each year from all seamounts to all nursery areas (c) The total connectivity for each year was computed at the end of the simulation (365 days since spawning) and the median was computed from annual averages for each of the twenty-two years simulated (1997-2018).

The connection between individual seamounts and nursery areas varied quite strongly inter-annually, and the deviation from the median was often of a similar magnitude to the median

(**Figure 9b**). Reflecting the median connectivity pattern, for all seamounts, the largest deviation about the median connectivity was to nursery area 6. Total connectivity (C_{TOT}) between all seamounts and any of the 12 alongshore nursery areas also varied interannually (**Figure 9c**) with no discernible trend over the time series. The maximum (C_{TOT}=10.4) occurred in 2018, following increasingly larger values in 2016 (C_{TOT}=8.4) and 2017 (C_{TOT}=9.8). Prior to this recent increase in connectivity, the largest connectivity (C_{TOT}=8.1) occurred in 2002. A minimum connectivity (C_{TOT}=4.2) occurred in 2013 with similarly low values (C_{TOT}=4.3) in 2001 and 2010. Over all years examined, the fraction of eggs that successfully settled as juveniles in any shallow nursery areas along the GOA coast (**Figure 10**) increased from a median of 0.21, for individuals 'spawned' over the Giacomini seamount (S13) at the far west of the chain, to a median of 0.57 for individuals 'spawned' over the S9. There was a slight decrease in the median fraction successful (~0.5) for M6-M8 followed by an increase to a maximum of 0.67 from S5 (the Welker Seamount). The fraction successful dropped to ~0.58 for individuals originating from M2-M4 and decreased again to a median of 0.44 for individuals spawned over S1 (the Hodgkins/Bowie complex) at the easternmost end of the chain.

The interquartile range (IQR) in fraction successfully settling over the model years examined was smallest (0.15) for S10 and S6 and ranged from 0.2-0.35 for the other seamounts. The size of the notches in the boxplots is indicative of the uncertainty in the value of the median and the bounds of the notches are determined by median±1.58*IQR/$\sqrt{n}$, where n is the sample size. Here n=22, the number of years in our study. It is generally accepted that lack of overlap in the notches of two boxes is evidence of a statistically significant difference (at a 95% confidence level) in their medians. (McGill *et al*., 1978). As the notch for S13 does not overlap with the notches determined for S1-S11 (Figure 10), we can conclude that the median likelihood of successful settlement to any of the alongshore nursery areas was significantly less for individuals spawned over seamount S13 than these other seamounts. Likewise, we can conclude that the median fraction successful from S5 is significantly higher than the median fraction successful from S1, S11, and S12.

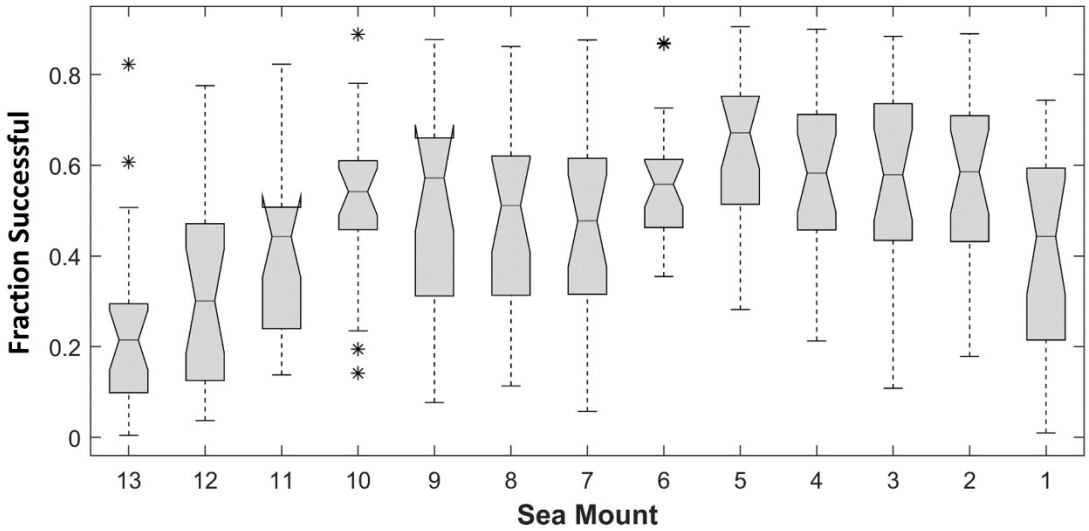

Figure 10. Boxplots showing the probability of individuals released over each seamount (S1-S13) settling in any alongshore nursery area. Values were computed for the twenty-two-year simulation period (1997-2018). The probability extremes are represented by the upper and

lower whiskers and computed as Q3+1.5*(Q3-Q1) and Q1-1.5*(Q3-Q1) respectively where Q1 is the 25th percentile and Q3 is the 75th percentile. Outlying data points, beyond the whiskers, are represented by an asterisk (*).

Annual deviations from median connectivity between individual seamounts and alongshore nursery areas (**Figure 11**) show that the change in the strength of the pairwise connections was not homogenous. In most years, some seamounts and nursery areas had a stronger than median connection, while others had a weaker than median connection. Years that saw a greater than median connectivity from the seamounts to nursery areas in the western GOA often had a weaker than median connectivity to the nursery areas in the eastern GOA. 2003 stands out as a year that had above median connectivity from most seamounts to most nursery areas. 2016-2018 were years that broadly exhibited much greater than average connectivity, although connectivity from some of the eastern seamounts was below average. The dominant patterns in relative connectivity between seamount and nursery area pairs throughout the 22-year study period are underscored in the EOF analysis (**Figure 12**). The first two EOFs of the annual connectivity matrix, which together accounted for 43.3% of the total variance, both show strong similarity in the strength of the connection from each seamount to each nursery area indicating that there is synchrony across the seamounts in the GOA seamount province to the nearshore environment. The first principal component of the EOF analysis (PC1) explained 27.8 % of the total variance while the second principal component (PC2) explained an additional 15.5 % of the total variance. In general, positive PC1 scores were associated with stronger connectivity from all seamounts to nursery areas in the eastern GOA (alongshore areas 1-6) but lower connectivity to the western GOA (along nursery shore areas 7-11). Positive PC1 scores were associated with increased connectivity between S12 and S13 at the far western end of the seamount chain and the nursery areas. Positive PC2 scores are associated with reduced connectivity to the east-central GOA, especially to nursery areas 4 and 5, but increased connectivity to the west-central GOA (i.e. nursery areas 7 and 8).

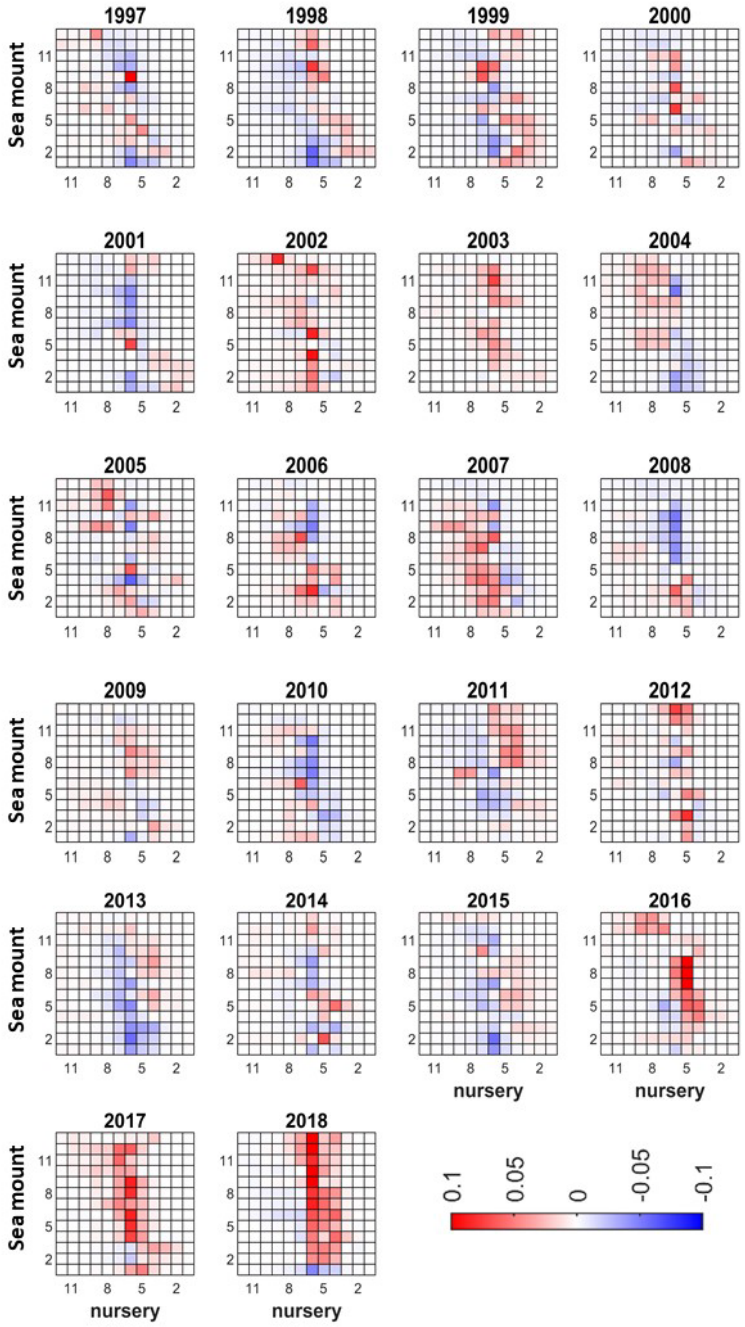

Figure 11. Annual deviations from the median connectivity for each seamount-nursery area pair. Red indicates above median connectivity while blue indicates below median connectivity.

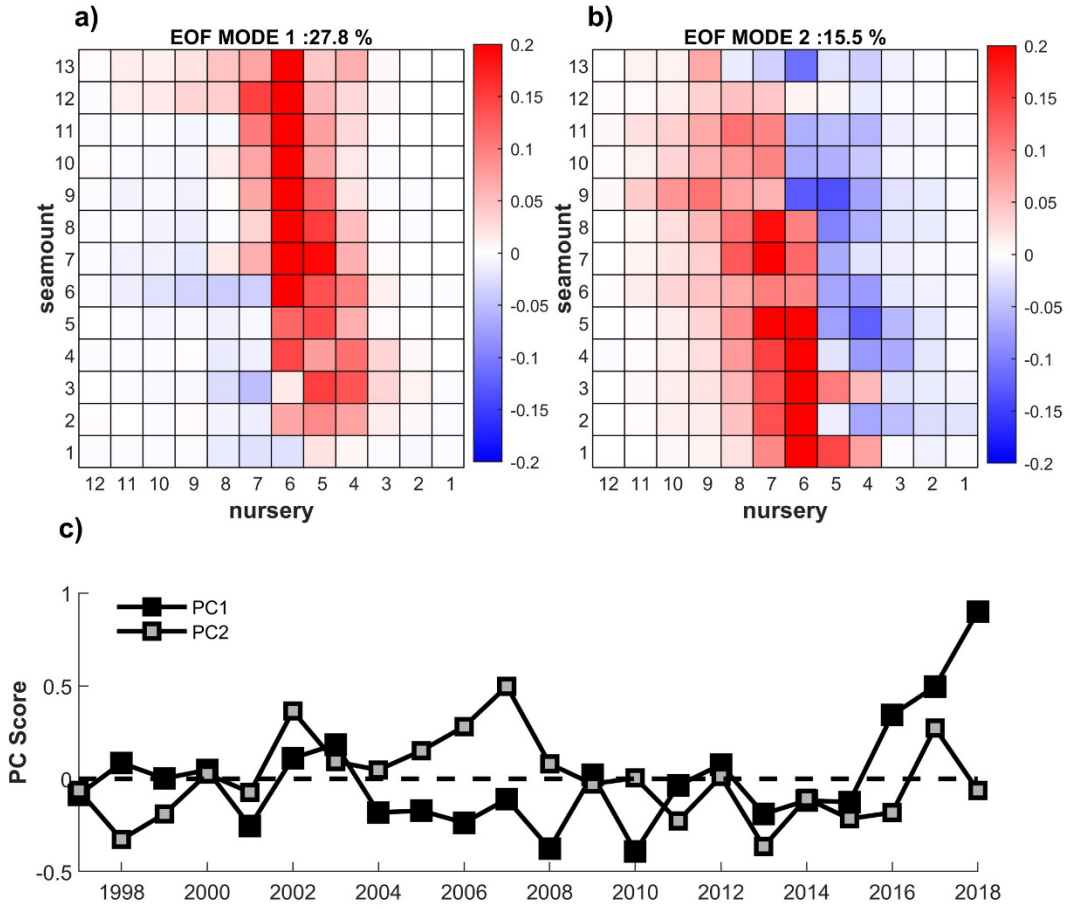

Figure 12. First (a) and second (b) mode spatial patterns from an EOF analysis of the annual mean probability of connection between the spawning area- nursery area pairs across the GOA for the 1997-2018 period. The corresponding 1st (black) and 2nd (grey) principal component time-series (PC) are shown in (c).

Path analysis visually illustrates that the dominant transport pathways for individuals that successfully settled also varied interannually (**Figure 13**). In 2002, a year that had relatively high total connectivity, a slightly positive PC1 (0.11) and a strongly positive PC2 (0.36) individuals spawned over the Welker seamount (S5), the seamount that had the largest fraction successful, were primarily transported directly north before taking a hard westward turn along the shelf break before traversing the shelf to the shallow nursery areas in the central gulf (**Figure 13a**). In 2007, a year with similarly high total connectivity but an even stronger positive PC2 (0.50) and a slightly negative PC1 (-0.11), individuals from S5 were initially transported to the north-west before sharply reversing direction to the southeast to pass M4 before eventually being transported northwards to the coast (**Figure 13b**); Individuals appear to primarily reach the coast in the vicinity of N5-N7. In 2009, a year of average connectivity and average PC1 (0.02) and PC2 (-0.03) scores there appears to be a bifurcated transport pathway with individuals being transported both northeast and southwest away from the seamount (**Figure 13c**); The individuals that were transported northwards appear to have been transported westwards in the shelf break current with no strong across shelf transport. Both 2010 and 2013 were years with low total connectivity. In 2010, PC1 was strongly negative (-0.39) but PC2 was average (0.01) while in

2013 both PC1 and PC2 were negative (-0.19 and -0.36 respectively). In both years the path analysis indicates that most individuals were trapped in eddies in the vicinity of the seamounts (**Figures 13 d and e**). Individuals that made it to a coastal settlement area did not follow a well-defined path. 2018 had the strongest total connectivity (10.4) of the years examined. While PC2 was slightly below average (-0.06) PC1 was strongly positive (0.9). While the initial transport away from the seamount was also bifurcated in this year, with concentrated transport both to the east and west (**Figure 13f**), most individuals were then transported northwards and crossed directly onto the shelf to reach the coast between N3 and N5.

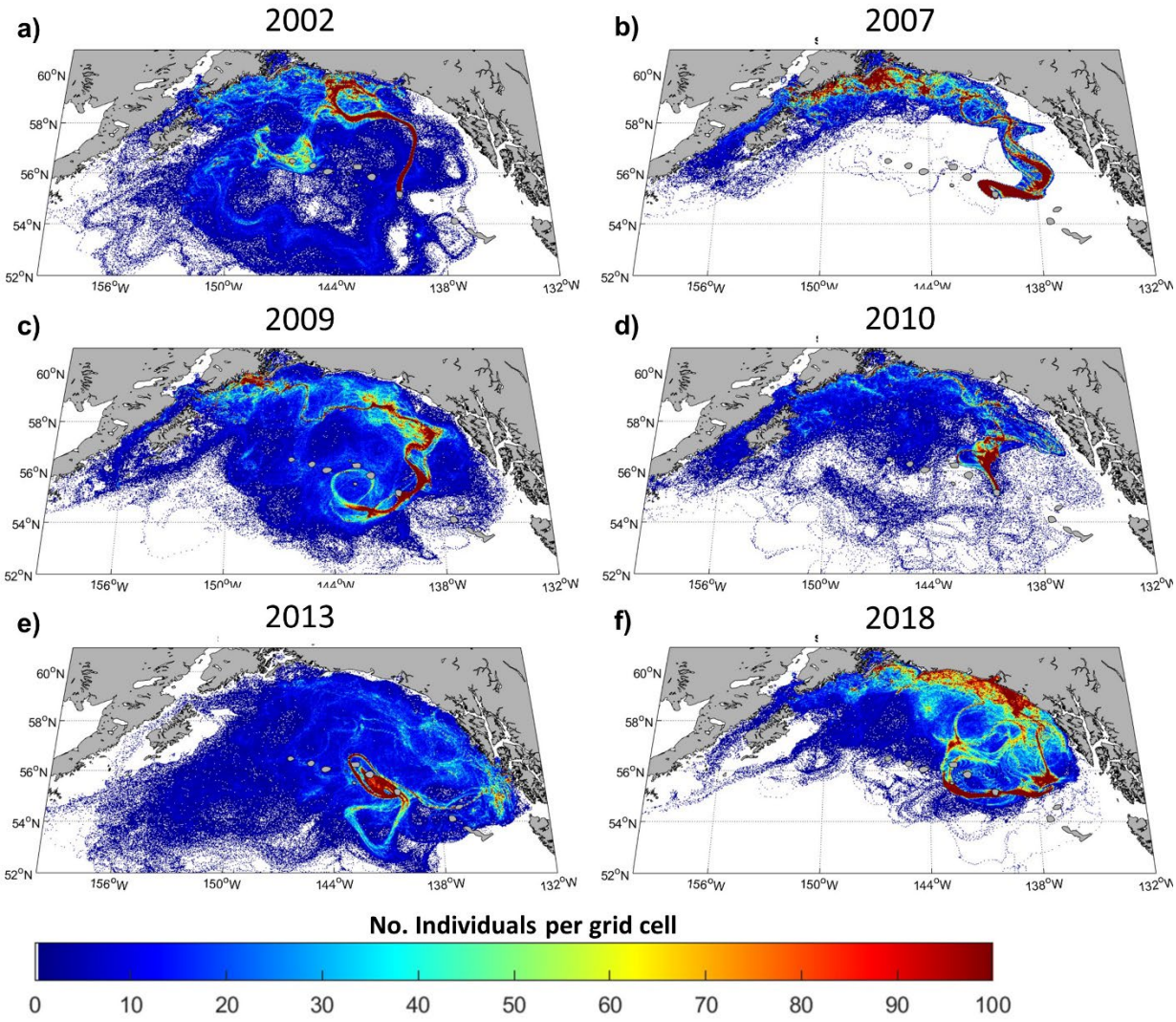

Figure 13. Path analysis shows the dominant pathways taken by individuals as they are transported away from the Welker seamount (S5). The count per grid cell is a sum of all individuals in a cell for each of the 365 days of the experiment.

Transport from the other seamounts in the chain also varied quite markedly interannually. For example, path analysis for seamount 1 indicates that in 2009, a year with average connectivity

and average PC1 and PC2, there was initially strong retention of the individuals around the easterly seamounts before transport on and across the shelf to coastal settlement areas **(Figure 14a)**; there was no strong transport from S13 to the settlement areas **(Figure 14b)**. In 2013, a year with low total connectivity, individuals from S1 appear to be initially retained south of the seamounts before being transported north-eastwards, towards the coast; however, there was no strong transport pathway across the shelf **(Figure 14c)**. In this year, individuals from S13 also appear to have been initially south of the seamount and were then broadly dispersed around the gulf with no clear transport coastwards **(Figure 14d)**. In 2018, the year with the strongest total connectivity, a transport pathway east then north from S1 to the coast is apparent **(Figure 14e)** while individuals from S13 were transported eastwards as far as S12 before taking multiple paths north to reach the coast **(Figure 14f).**

The survival of individuals from one life stage to the next varied by seamount spawning site and year. Even in years with high overall connectivity to the inshore nursery sites, individuals from some seamounts had low survival. For example, in 2018, the year with the highest overall connectivity, only 26% of the eggs released from S1, the Hodkins-Bowie complex, successfully transitioned to the yolk-sac larval stage (**Figure 15**) and only 10% transitioned to the feeding larvae stage. Examination of the individual life histories indicates that this is because the individuals were lost from the system via advection to the east and out of the model domain. In 2010, a year with relatively low connectivity between seamounts and nursery areas most individuals (>96%) successfully transitioned through to the feeding larvae stage (**Figure 15**). However, only 58% of individuals initiated over S13 transitioned to epi-pelagic juveniles and only 35% transitioned to juveniles. Examination of these life histories reveals that this was due to the individuals being transported out of the system through the western edge of the model grid.

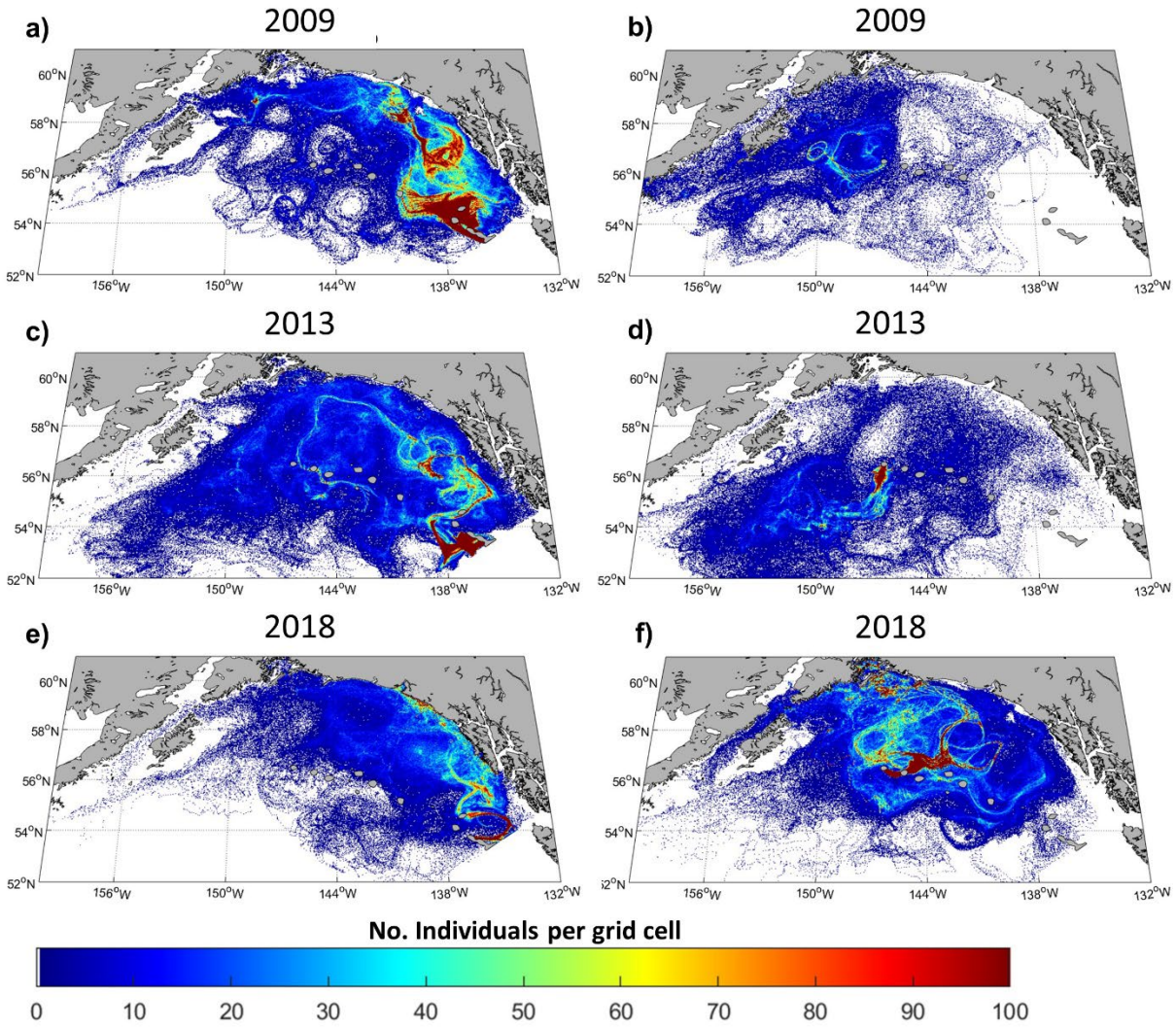

Figure 14. Path analysis showing the transport pathways taken by individuals as they are transported away from the Hodgkins-Bowie complex (S1) at the eastern end of the seamount chain (a, c, e) and the Giacomini seamount (S13) at the western end of the chain (b, d, f). The count per grid cell is a sum of all individuals in a cell for each of the 365 days of the experiment.

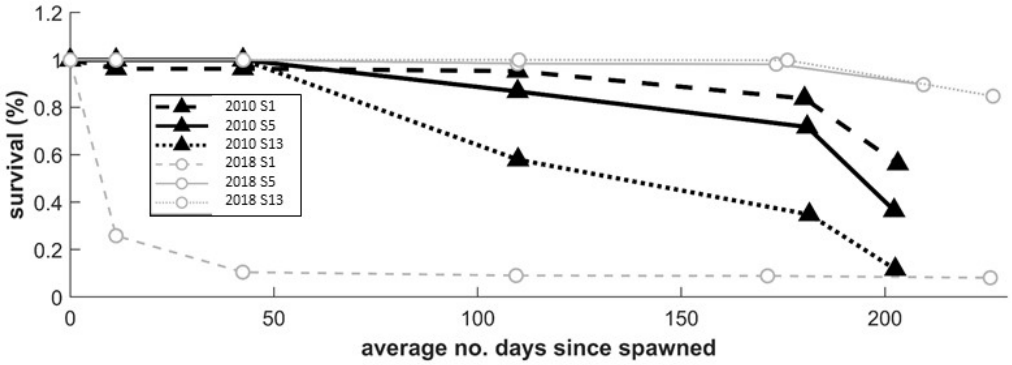

Figure 15. Fraction of individuals surviving to each life stage transition for individuals released from seamount S1 (Hodkins-Bowie), S5 (Welker), and S13 (Giacomini) in 2010 and 2018.

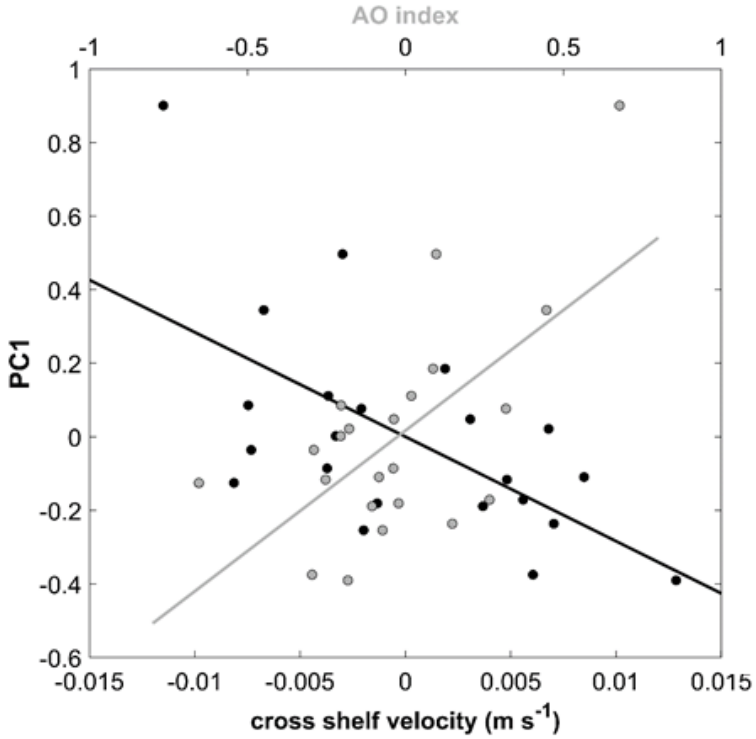

Figure 16. Relationship between PC1 and annual average cross-shelf velocity (r=-0.62, p=<0.01) in the eastern Gulf of Alaska (135°-140 °W, black points and line) and PC1 and the July-September Arctic Oscillation index (r= 0.64, p=<0.01, grey points and line).

The PC1 time series from our EOF analysis of the connectivity matrices were negatively correlated (*r*=0.62 respectively) with the annual average on-shelf flow in the Eastern GOA (**Table 2, Figure 16**). No significant correlations were found between PC1 and on-shelf flow in other regions or seasons (**Table 2)**. The average temperature and salinity along the 500m isobath in each season and domain in the GOA also showed no relationship to PC1. We found a positive

709 correlation between both PC1 (r=0.64) and C_{TOT} (r=0.69) and the AO time series for the summer
710 (July-September) time period (**Figure 16**). No significant correlations were found between either
711 metric and the AO for other seasons, and no relationship was found between C_{TOT} and on-shelf
712 velocity or temperature in any season.
713
714 **4. Discussion**
715 Using an IBM of sablefish, we have demonstrated that if sablefish were spawned over any of the
716 seamounts in the GOA seamount province it is likely that at least some individuals will be
717 successfully transported to shallow inshore nursery areas in the coastal GOA. Due to their
718 distance from shore, sampling over the seamounts is relatively rare. However, females that have
719 recently spawned, or are ready to spawn, have been observed over the seamounts (Maloney,
720 2004) which has raised the questions of the role of these geographic features in sablefish life
721 history. Here we have shown that larval transport hundreds of miles from the seamounts to
722 suitable nursery habitat along the Gulf of Alaska coast within an appropriate timeframe is not
723 only possible, but likely. Our simulated individuals currently only exhibit vertical movement
724 behavior, thus the predicted on-shore transport results from the prevailing currents and not due to
725 any geographic or environmental homing capabilities.
726
727 In general, the strongest connection from each of the seamounts in the chain was to the central
728 GOA nursery areas. While in some years juvenile sablefish are found in nursery habitats all
729 along the GOA coast, often their nursery areas are thought to be more restricted. For example,
730 juvenile sablefish are consistently found in St. John Baptist Bay (SJBB) in Southeast Alaska.
731 While a small percentage of individuals released over the seamounts at the eastern end of the
732 chain were transported to nursery areas near SJBB (alongshore nursery areas three), it was not a
733 dominant mode of connectivity. An earlier version of the sablefish IBM (Gibson *et al*., 2019)
734 indicated that transport to this bay is also not the most likely outcome for individuals spawned
735 over the continental shelf. This led the authors to hypothesize that individuals settling in SJBB
736 were either taking advantage of sub-mesoscale physical transport mechanisms not captured by
737 the model, or they were originating from source areas to the south of the model domain – i.e. off
738 of the coast of Washington. Connectivity between most seamounts and inshore areas was not
739 significantly different and EOF analysis found that connectivity from the seamounts tends to
740 vary in unison. The connectivity from the westernmost seamount in the chain (S13) was
741 significantly less than for most of the other seamounts. It is likely that individuals 'spawned'
742 over this far western seamount exited the GOA to the west, as was the case for individuals
743 spawned off of the western GOA shelf break in an earlier version of the model (Gibson *et al*.,
744 2019).
745
746 It is not typical for research surveys to extend much beyond the continental shelf break due to
747 time and logistical constraints. However, in addition to the limited evidence of adult sablefish
748 spawning over the seamounts (Maloney 2004), juvenile sablefish have been observed close to the
749 seamounts on a few occasions. During a research cruise in the eastern GOA that occurred July-
750 August 2016, age-0 sablefish were found beyond the shelf break (Strasburger, *et al.,* 2018), in
751 the vicinity of seamounts; however, it was not known where these individuals originated from. A
752 much older research cruise in the eastern GOA during May 1990 (Wing and Kamikawa, 1995)
753 also found the highest catches of sablefish larvae to be 160km offshore, beyond the shelf break
754 near the seamounts. The authors attributed their presence to offshore transport resulting from the

absence of the Haida and Sitka eddies, as well as an absence of the more typical downwelling system that is often found in the region.

While the prevailing oceanography across the GOA plays a crucial role in the onshore transport of individuals that were spawned over the seamounts our results show that the strength of the cross-shelf velocity is not the primary factor in determining the likelihood of transport to nursery areas. Both total connectivity and the 1st PC for connectivity (PC1) between the seamounts and the inshore nursery areas was negatively correlated with the annual averaged on-shelf velocity in the eastern GOA and no other correlations between seasonal or annually-averaged on-shelf velocity could be found. In 2018, the year with the strongest simulated connectivity, the on-shelf velocity in the east was the lowest of all years examined. Path and survival analysis indicates that in this year individuals from the western end of the seamount chain were transported east and retained in the GOA where they could successfully transition through the early life stages becoming juveniles with the ability to settle, rather than being advected out of the system to the west, as is more typical. A positive correlation between PC1 and the AO index suggests that the mechanisms impacting the transport of individuals from the seamounts to the inshore areas could be acting on a gulf-wide scale. We speculate that the size, strength, location, and direction of the eddies that populate the GOA (i.e. Appendix A) in any given year, and the temporal and spatial alignment of these features with sablefish early life history, are important in determining transport success. Indeed, Shotwell *et al*. (2014) discussed that young of the year (YOY) sablefish entering surface waters may be entrained in coastally-derived eddies translating along the shelf-break. Similarly, Goldstein *et al*. (2020) found that cross-shelf transport and settlement of Arrowtooth flounder in the GOA was augmented by transient retentive mesoscale eddies. Anticyclonic eddies may become trapped as they translate along the shelf-break through the Alaskan Stream eddy corridor during periods of increased circulation (Henson and Thomas, 2008). This may increase the entrained nutrients in a given area and allow for more productive waters and transport of larval fish along the eddy path (Atwood *et al*., 2010). The timing of these mesoscale features can be short or long-lived (Okkonen *et al*., 2003; Ladd *et al*., 2007) and it could simply be a matter of luck as to whether the timing of sablefish spawning coincides with the favorable transport by an eddy. This idea is reinforced by the large deviation about median connectivity and by our path analysis which shows that there are markedly different pathways taken by successful individuals year on year.

Sablefish recruitment is defined as the number of age-2 sablefish entering the population as estimated in the stock assessment model (Hanselman *et al*., 2014). Past analysis (Gibson *et al*., 2019) found that the total connectivity between all potential sablefish spawning sites along the GOA continental shelf and inshore nursery areas showed a stronger correlation with recruitment estimates than the strength of connections to or from specific regions. While we have not directly related the connectivity from seamount sites to recruitment, it is worth noting that the most recent years for which recruitment estimates are available (2018 through 2020) correspond to simulation years with strong connectivity two years prior (2016 through 2018) when the individuals would have been in the larval stage and being transported onto the shelf (Goethel *et al*., 2021). We speculate that the increase in recruitment could be related to an increase in seamount-spawned individuals reaching favorable settlement areas. The ecosystem and socioeconomic profile (ESP) associated with the sablefish stock assessment (Goethel *et al*., 2021, cf. Appendix 3C,) provides a series of indicators for monitoring ecosystem linkages to the

stock. The sablefish ESP states that catch per unit effort of sablefish in nearshore surveys along the western GOA and the Aleutian Islands has been the highest in the time series over the years 2018 to 2021 approximately corresponding to sablefish year classes from 2015 to 2018. Catch per unit effort of sablefish has also increased in the sablefish targeted pot fishery and incidental catch has increased in the non-sablefish target fisheries of the eastern Bering Sea since 2016. All three indicators support the idea of higher connectivity years, demonstrated in this analysis, and also suggest that the sablefish can utilize different habitats when their population expands or environmental conditions change.

As noted earlier, the connectivity from the western GOA (both seamount and slope region) was lower than other areas investigated and likely due to individuals exiting the system. Verification of this distribution shift into the Aleutian Islands and the eastern Bering Sea due to connectivity increases and contributions of the seamounts in the most recent years could be possible if these individuals were able to be tracked further into these areas. This type of exploration would require an expansion of the 3km ROMS GOA model past the western boundary through the Aleutian Islands and into the Bering Sea. If a continuous ROMS model were developed for the whole Alaska region, we would be able to test such linkages and also develop more relevant indicators for the management of the fishery in either the sablefish ESP or for use specifically in the stock assessment model.

The spawning center for sablefish has historically been thought to be in deep water over the GOA continental shelf. If the seamounts do indeed play a role in the life history of the species it may be useful to consider the potential contribution of the seamount habitat to the sablefish population. While we have demonstrated that if sablefish did spawn over the seamounts, transport to coastal nursery areas is likely, we acknowledge the present limits of our understanding as to the contribution of the seamount population to the sablefish population as a whole. To address this question would require a true measure of the spawning biomass on the seamounts to compare potential contributions of recruits relative to the contribution by the more consistently monitored slope population. Sablefish are managed in Alaska using a harvest control rule that aims to preserve sufficient spawning biomass. With seamounts being a potentially important spawning site for sablefish this presents future research priorities for ground-truthing with fishery or fishery-independent data. Sampling for YOY sablefish has been conducted in the past (Sigler *et al*., 2001, Strasburger *et al*., 2018) including tagging of YOY (Strasburger *et al*., 2018). Tag recovery information from larval sablefish tagged in the vicinity of the seamount areas would be valuable, although technically challenging due to their small size, in validating our findings and represents a research priority that would help evaluate the importance of seamounts to sablefish populations in the Pacific.

Information on connectivity from this IBM could also be used to inform the movement of sablefish during their first year of life within a spatially integrated life cycle model that is in development for Alaska sablefish (Goethel *et al*., 2021). This type of stock assessment model could be used to generate regional estimates of recruitment that can then be linked with relevant environmental indicators as explored in the ESP to understand spatial shifts in the sablefish population. Explorations of alternative habitats and hypotheses regarding the designation of stock distributions used in management, such as the use of seamounts for Alaska sablefish, may become more important with increased environmental variability due to climate change. This study provides an example of utility for IBMs in testing habitat expansions or distributional

shifts and contributing to next-generation stock assessments (Lynch *et al*., 2018).

Acknowledgments

This publication is the result in part of research sponsored by the Cooperative Institute for Alaska Research with funds from the National Oceanic and Atmospheric Administration under cooperative agreement NA13OAR4320056 with the University of Alaska. Additional support for this research was provided through the North Pacific Research Board (NPRB) Gulf of Alaska Integrated Ecosystem Research Program Synthesis Project #1533 (https://www.nprb.org/gulf-of-alaska-project), the Joint Institute for the Study of the Atmosphere and Ocean (JISAO) under NOAA Cooperative Agreement NA15OAR4320063, and the National Marine Fisheries Service (NMFS), and the NMFS Alaska Essential Fish Habitat Research Plan. The findings and conclusions in the paper are those of the authors and do not necessarily represent the views of the National Marine Fisheries Service. Reference to trade names does not imply endorsement by the National Marine Fisheries Service, NOAA.

References

Alderdice, D.F., Jensen, J.O.T., and Velsen, F.P.J., 1988. Preliminary trials on incubation of sablefish eggs. Aquaculture. 69, 271–290.

Alton, M.S., 1986. Fish and crab populations of Gulf of Alaska seamounts. In R. N. Uchida, S. Hayasi, and G. W. Boehlert (editors), Environment and resources of seamounts in the North Pacific, U.S. Dep. Commerce, NOAA Tech. Rep. NMFS 43. pp. 45–51.

Atwood, E., Duffy-Anderson, J.T., Horne, J.K., and Ladd, C., 2010. Influence of mesoscale eddies on ichthyoplankton assemblages in the Gulf of Alaska. Fish. Oceanogr. 19(6), 493-507.

Beamish, R.J., and McFarlane, G.A., 1988. Resident and dispersal behavior of adult sablefish (Anoplopoma fimbria) in the slope waters off Canada's west coast. Canadian Journal of Fisheries and Aquatic Sciences. 45, 152–164.

Beamish, R.J., and Neville, C.M., 2003. The importance of establishing Bowie Seamount as an experimental research area. In: Beumer, J., Grant, A., Smith, D. (Eds.), Aquatic Protected Areas: What Works Best and How do We Know? Proceedings of the World Congress on Aquatic Protected Areas, Cairns, Australia, August 2002, Australian Society for Fish Biology. North Beach, Australia, pp. 652–663.

Beamish, R.J., and McFarlane, G.A., 1983. Summary of results of the Canadian sablefish tagging program. In: Proceedings of the International Sablefish Symposium, March 29–31, 1983, Anchorage, AK, pp. 147–183. Alaska Sea Grant Report. 83-8

Boehlert, G.W. and Yoklavich, M.M., 1985. Larval and Juvenile growth of sablefish, Anoplopoma Fimbria, as determined from otolith increments. Fishery Bulletin. 83, No.3, 475-481.

Bracken, B.E., 1982. Sablefish (Anoplopoma fimbria) migration in the Gulf of Alaska based on gulf-wide tag recoveries, 1973-1982. Alaska Department of Fish and Game. Informational Leaflet No. 199.

Castro-Gutiérrez, J., Cabrera-Castro, R., Czerwinski, I.A. Báez, José, C. 2022. Effect of climatic

oscillations on small pelagic fisheries and its economic profit in the Gulf of Cadiz. Int J Biometeorol. 66, 613–626.
Cheng, W., Hermann, A.J., Coyle, K.O., Dobbins, E.L., Kachel, N.B., and Stabeno, P.J., 2012. Macro- and micro-nutrient flux to a highly productive submarine bank in the Gulf of Alaska: A model-based analysis of daily and interannual variability. Prog. Oceanogr. 101, 63–77.
Cook, M. A., Lee, J.S.F, Massee, K.M., Wade, T.H., and Goetz, F.W., 2017. Effects of rearing temperature on growth and survival of larval sablefish (Anoplopoma fimbria). Aquaculture Research. 49. 10.1111/are.13473.
Cooper, D.W., Duffy-Anderson, J.T., Stockhausen, W.T., and Cheng, W., 2013. Modeled connectivity between northern rock sole (Lepidopsetta polyxystra) spawning and nursery areas in the eastern Bering Sea. J. Sea Res. 84, 2–12.
Courtney, D., and Rutecki, T.L., 2011. Inshore movement and habitat use by juvenile sablefish, Anoplopoma fimbria, implanted with acoustic tags in southeast Alaska, AFSC Processed Report 2011-01, 39 p. Alaska Fish. Sci. Cent., NOAA, Natl. Mar, Fish. Serv., Auke Bay Laboratories,17109 Lena Point Loop Road Juneau, AK 99801.
Coyle, K.O., Gibson, G. A., Hedstrom, K., Hermann, A. J., and Hopcroft, R.R., 2013. Zooplankton biomass, advection and production on the northern Gulf of Alaska shelf from simulations and field observations. J. Mar. Syst. 128, 185–207.
Coyle, K.O., Hermann, A.J. and Hopcroft, R.R., 2019. Modeled spatial-temporal distribution of productivity, chlorophyll, iron and nitrate on the northern Gulf of Alaska shelf relative to field observations. Deep Sea Research Part II: Topical Studies in Oceanography. Volume 165, 163-191.
Danielson, S. L., Dobbins, E. L., Jakobsson, M., Johnson, M. A., Weingartner, T. J., Williams, W. J., and Zarayskaya, Y., 2016. Sounding the northern seas, Eos, 96.
Danielson, S.L., Hill, D.F., Hedstrom, K.S., Beamer, J. and Curchitser, E., 2020. Demonstrating a high-resolution Gulf of Alaska ocean circulation model forced across the coastal interface by high-resolution terrestrial hydrological models. Journal of Geophysical Research: Oceans, 125(8), p.e2019JC015724.
Deary, A.L., Porter, S.M., Dougherty, A.B. and Duffy-Anderson, J.T., 2019.Preliminary observations of the skeletal development in pre-flexion larvae of sablefish Anoplopoma fimbria. Ichthyol Res. 66, 177–182.
DFO, 2013. A Review of Sablefish Population Structure in the Northeast Pacific Ocean and Implications for Canadian Seamount Fisheries. DFO Can. Sci. Advis. Sec. Sci. Resp. 2013/017.
Dobbins, E.L., Hermann, A.J., Stabeno, P., Bond, N. A., and Steed, R.C., 2009. Modeled transport of freshwater from a line-source in the coastal Gulf of Alaska. Deep. Res. Part II Top. Stud. Oceanogr. 56, 2409–2426.
Doyle, M.J., and Mier, K.L., 2015. Early life history pelagic exposure profiles of selected commercially important fish species in the Gulf of Alaska. Deep-Sea Res. II.
Fissel, B., Dalton, M., Felthoven, R., Garber-Yonts, B., Haynie, A., Kasperski, S., Lee, J., Lew, D., Pfeiffer, and L., Seung, C., 2012. Stock Assessment and Fishery Evaluation Report for the Groundfish Fisheries of the Gulf of Alaska and Bering Sea/Aleutian Islands Area: Economic status of the groundfish fisheries off Alaska, 2011, 309 p.
Flanders Marine Institute (2019). Maritime Boundaries Geodatabase: Maritime Boundaries and Exclusive Economic Zones (200NM), version 11. Available online at

https://www.marineregions.org/. https://doi.org/10.14284/386

Funk, F., and Bracken, B.E., 1984. Status of the Gulf of Alaska Sablefish (Anoplopoma fimbria) resource in 1983. Informational Leaflet No. 235. Alaska Department of Fish and Game Division of Commercial Fisheries Juneau, A1aska 55 p.

Gibson, G.A. Stockhausen, W., Coyle, K.O., Hinckley, S., Parada, C., Hermann, A., Doyle, M. and Ladd, C., 2019. An individual-based model for Sablefish: Exploring the connectivity between potential spawning and nursery grounds in the Gulf of Alaska. Deep Sea Res. II. 165, 89–112.

Goethel, D.R., Hanselman, D.H., Rodgveller, C.J., Echave, K.B., Williams, B.C., Shotwell, S.K., Sullivan, J.Y., Hulson, P.F., Malecha, P.W., Siwicke, K.A., and Lunsford, C.R., 2021. Assessment of the Sablefish Stock in Alaska. In Stock assessment and fishery evaluation report for the groundfish resources of the Gulf of Alaska and Bering Sea Aleutian Islands. North Pacific Fishery Management Council, 605 W 4th Ave, Suite 306 Anchorage, AK 99501.

Goldstein, E. D., Pirtle, J. L., Duffy-Anderson, J. T., Stockhausen, W. T., Zimmermann, M., Wilson, M. T., Mordy, C.W. (2020). Eddy retention and seafloor terrain facilitate cross-shelf transport and delivery of fish larvae to suitable nursery habitats. *Limnology and Oceanography* 65, 2800–2818. doi: 10.1002/lno.11553.

Hanselman, D.H., Lunsford, C.R., and Rodgveller, C.J., 2014. Assessment of the sablefish stock in Alaska, in: Stock Assessment and Fishery Evaluation Report for the Groundfish Resources of the Gulf of Alaska. North Pacific Fishery Management Council, 605W. 4th Avenue, Suite 306, Anchorage, AK 99501, pp. 576–717.

Hanselman, D.H., Heifetz, J., Echave, K.B., and Dressel, S.C., 2014b. Move it or lose it : movement and mortality of sablefish tagged in Alaska. Can. J. Fish. Aquat. Sci. 72(2), 238–251.

Hart, J.L., 1973. Pacific fishes of Canada. Bull. Fish. Res. Bd. Can. 180, 740 p.

Heifetz, J., and Fujioka, J.T., 1991. Movement dynamics of tagged sablefish in the northeastern Pacific. Fisheries Research. 11(3–4). 355–374.

Henson, S.A., and Thomas, A.C., 2008. A census of oceanic anticyclonic eddies in the Gulf of Alaska. Deep-Sea Res. I, 55. 163-176.

Herzer, R.H. (1971) Bowie Seamount. A Recently Active, Flat-topped Seamount in the Northeast Pacific Ocean. Can. J. Earth Sci. 8. 676-687.

Hermann, A.J., Hinckley, S., Dobbins, E.L., Haidvogel, D.B., Bond, N.A., Mordy, C., Kachel, N., and Stabeno, P.J., 2009. Deep-Sea Research II Quantifying cross-shelf and vertical nutrient flux in the Coastal Gulf of Alaska with a spatially nested , coupled biophysical model. Deep-Sea Res. Part II 56, 2474–2486.

Hinckley, S., Stockhausen, W.T., Coyle, K.O., Laurel, B. Gibson, G.A., Parada, C. Hermann, A.J., Doyle, M., Hurst, T., Punt, and A. Ladd, C., 2019. Connectivity between spawning and nursery areas for Pacific cod (Gadus macrocephalus) in the Gulf of Alaska. Deep Sea Res. II. 165,113–126.

Hinckley, S., Coyle, K.O., Gibson, G., Hermann, A. J., Dobbins, E.L., 2009. A biophysical NPZ model with iron for the Gulf of Alaska: Reproducing the differences between an oceanic HNLC ecosystem and a classical northern temperate shelf ecosystem. Deep-Sea Res. Part II Top. Stud. Oceanogr. 56, 2520–2536.

Hoff, G.R. and Stevens, B., 2005. Faunal Assemblage Structure on the Patton Seamount (Gulf of Alaska, USA). Alaska Fisheries Research Bulletin. Vol. 11, No. 1

Hughes, S.E., 1981. Initial U.S. Exploration of Nine Gulf of Alaska Seamounts and Their Associated Fish and Shellfish Resources Marine Fisheries Review. 43(1).

Hunter, J.R., Macewicz, B.J., and Kimbrell, C. A., 1989. Fecundity and other aspects of the reproduction of sablefish, Anoplopoma fimbria, in central California waters. CalCOFI Rep. 30, 61–72.

Jensen, J. O. T., and Damon, W., 2002. Digital photo-microscopy of sablefish (Anoplopoma fimbria) embryonic development. In J. Jensen, C. Clark, & D. M. Kinlay (Eds.), Incubation of fish: biology and techniques (pp. 49– 58). Vancouver, Canada: International Congress on the Biology of Fish.

Kapur, M. S., Lee, Q., Correa, G. M., Haltuch, M., Gertseva, V., and Hamel, O. S., 2021. DRAFT Status of Sablefish (Anoplopoma fimbria) along the US West coast in 2021. Pacific Fisheries Management Council, Portland, Oregon. 136p.

Kendall, A.W. and Matarese, A., 1987. Biology of eggs , larvae , and epipelagic juveniles of sablefish , Anoplopoma fimbria, in relation to their potential use in management. Marine Fisheries Review. 49, 1–13.

Kimura, D.K., Shimada, A.M., and Shaw, F.R., 1998. Stock structure and movement of tagged sablefish, Anoplopoma fimbria, in offshore northeast Pacific waters and the effects of El Niño-Southern Oscillation on migration and growth. Fish. Bull. 96, 42-481.

Ladd, C., Mordy, C.W., Kachel, N.B., Stabeno, P.J., 2007. Northern Gulf of Alaska eddies and associated anomalies. Deep-Sea Res. I, 54, 487-509.

Leys, C., Ley, C., Klein, O., Bernard, P. Licata, L. (2013) Detecting outliers: Do not use standard deviation around the mean, use absolute deviation around the median. Journal of Experimental Social Psychology. Volume 49, Issue 4, 764-766.

Lynch, P.D., Methot, R.D., and Link, J.S., (eds.), 2018. Implementing a Next Generation Stock Assessment Enterprise. An Update to the NOAA Fisheries Stock Assessment Improvement Plan. U.S. Dep. Commer., NOAA Tech. Memo. NMFS-F/SPO-183, 127 p. doi:10.7755/TMSPO.183

Maloney, N.E. and Sigler, M.F. 2008. Age-specific movement patterns of sablefish (Anoplopoma fimbria) in Alaska. Fish. Bull. 106, 305-316.

Maloney, N.E., 2004. Sablefish, Anoplopoma fimbria, populations on Gulf of Alaska seamounts. Mar. Fish. Rev. 66, 1–12.

Marquez, R.I., 2020. Fisheries of the Exclusive Economic Zone off Alaska; North Pacific Observer Program Standard Ex-Vessel Prices. Federal Register. 85, No. 244, 82447-82455.

Mason, J. C., Beamish, R. J., and McFarlane G. A., 1983. Sexual Maturity, Fecundity, Spawning, and Early Life History of Sablefish (Anoplopoma fimbria) off the Pacific Coast of Canada. Canadian Journal of Fisheries and Aquatic Sciences. 40(12), 2126-2134.

Mason, J.C., Beamish, R.J., McFarlane, G.A., 1983. Sexual maturity, fecundity, and early life history of sablefish (Anoplopoma fimbria) off the Pacific Coast of Canada. Can. J. Fish. Aquat. Sci. 40, 2126–2134.

McGill, R. Tukey, J.W. and Larsen, W.A., 1978. Variations of Box Plots, The American Statistician. 32(1), 12-16

Moser, H.G., Chakter, R.L., Smith, P.E., Lo, N.C.H., Ambrose, D.A. Meyer, C.A., Sandknop, E.M. and Watson, W., 1994. Sablefish early life history and Biomass estimation. CalCOFl Rep., Vol. 35.

Murie, D.J., Mitton, M., Saunders, M.W., and McFarlane, G.A., 1995. A summary of sablefish tagging and biological studies conducted during 1982-198 by the Pacific Biological Station.

Can. Data Rep. Fish. Aquat. Sci. 959: 84p.
National Marine Fisheries Service (NMFS). 2006. Final Rule: Fisheries of the Exclusive Economic Zone off Alaska. Federal Register 71 (124), 36694-36714. Codified at 50 CFR Part 679.
Okkonen, S.R., Weingartner, T.J., Danielson, S.L., Musgrave, D.L., Schmidt, G.M., 2003. Satellite and hydrographic observations of eddy-induced shelf-slope exchange in the northwestern Gulf of Alaska. J. Geophys. Res., 108(C2), 3033.
Pirtle, J.L., Shotwell, S.K., Zimmermann, M., Reid, J.A., and Golden, N., 2019. Habitat suitability models for groundfish in the Gulf of Alaska, Deep Sea Research Part II: Topical Studies in Oceanography. 165, 303-321.
Royer, T. C. (1979). On the effect of precipitation and runoff on coastal circulation in the Gulf of Alaska. Journal of Physical Oceanography, 9(3), 555– 563.
Rutecki, T.L., and Varosi, E.R., 1997. Distribution, age, and growth of juvenile sablefish, Anoplopoma fimbria, in the Gulf of Alaska, pp. 55–63, in: Wilkins, M.E., Saunders, M.W. (eds.), Biology and Management of Sablefish, Anoplopoma fimbria. U.S. Dep. Commer., NOAA Technical Report NMFS-130, 286 p.
Sasaki, T., 1985. Studies on the sablefish resources of the North Pacific Ocean. Bull. Far Seas Fish. Res. Lab. 22, 107.
Shaw, F., and N. Parks. 1997. Movement patterns of tagged sablefish recovered on seamounts in the N.E. Pacific Ocean and Gulf of Alaska. In M. E. Wilkins and M. W. Saunders (Editors), Biology and management of sablefish, Anoplopoma fimbria, p. 151–158. U.S. Dep. Commer., NOAA Tech Rep. NMFS 130.
Shotwell, S.K., Hanselman, D.H., Belkin, I.M., 2014. Toward biophysical synergy: Investigating advection along the Polar Front to identify factors influencing Alaska sablefish recruitment. Deep-Sea Res. Part II Top. Stud. Oceanogr. 107, 40–53.
Shotwell, S.K., Pirtle, J.L., Watson, J.T., Deary, A.L., Doyle, M.J., Barbeaux, S.J., Dorn, M. Gibson, G.A., Goldstein, E., Hanselman, D.H., Hermann, A.J., Hulson, P.J.F., Laurel, Moss, B.J.H. , Ormseth, O., Robinson, D., Rogers, L.A., Rooper, C.N., Spies, I., Strasburger, W., Suryan, R.M., and Vollenweider, J.J., 2022. Synthesizing integrated ecosystem research to create informed stock-specific indicators for next generation stock assessments. Deep Sea Research Part II: Topical Studies in Oceanography. 198.
Sigler, M.F., Rutecki, T.L., Courtney, D.L., Karinen, J.F., and Yang, M.-S., 2001. Young of the year sablefish abundance, growth, and diet in the Gulf of Alaska. Alaska Fish. Res. Bull. 8, 57–70.
Sogard, S., and Olla, B., 2001. Growth and behavioral responses to elevated temperatures by juvenile sablefish Anoplopoma fimbria and the interactive role of food availability. Mar. Ecol. Prog. Ser. 217, 121–134.
Stockhausen, W.T., Coyle, K.O., Hermann, A.J., Doyle, M., Gibson, G.A., Hinckley, S. Ladd, C., and Parada, C., 2019. Running the Gauntlet: Connectivity between natal and nursery areas for Pacific ocean perch (Sebastes alutus) in the Gulf of Alaska, as inferred from a biophysical Individual-based Model. Deep Sea Res. II. 165, 74–88.
Strasburger, W. W., Moss, J. H. Siwicke, K. A. and Yasumiishi, E. M., 2018. Results from the eastern Gulf of Alaska ecosystem assessment, July through August 2016. U.S. Dep. Commer., NOAA Tech. Memo. NMFS-AFSC-363, 90 p.
Thompson, D. W. J., and J. M. Wallace, 1998. The Arctic Oscillation signature in the winter geopotential height and temperature fields, Geophys. Res. Lett., 25, 1297–1300.

Whitaker, D.J., and McFarlane, G.A., 1997. Identification of Sablefish, Anoplopoma fimbria (Pallas, 1811), Stocks from seamounts of the Canadian Pacific Coast using parasites as biological tags. N.O.A.A. Technical Report, National Marine Fisheries Service 130, 131–136.

Wing, B. L., and Kamikawa. D. J., 1995. Distribution of neustonic sablefish larvae and associated ichthyoplankton in the eastern Gulf of Alaska, May 1990. U.S. Dep. Commer., NOAA Tech. Memo. NMFS- AFSC-53, 48 p.

Wolotira, R.J.J., Sample, T.M., Noel, S.F., and Iten, C.R., 1993. Geographic and bathymetric distributions for many commercially important fishes and shellfishes off the west coast of North America, based on research survey and commercial catch data, 1912-1984. U.S. Dept. Commer., NOAA Technical Memorandum NMFS-AFSC-6, 184 p.

Zolotov, A.O., 2021. The Long-Term Dynamics of Sablefish (Anoplopoma fimbria) Stocks in the Western Bering Sea and Prospects for their Commercial Exploitation. Russ J Mar Biol 47, 563–582.

Table 1. Summary of number of individuals released over each seamount, and the seamount area determined at a bathymetric depth of 2,500m.

Seamount No.	Seamount Name	Area at 2500m below sea level.	No. Individuals
1	Hodgkins-Bowie	1864	44,904
2	-	598	14,376
3	Dickens	459	11,040
4	-	68	1,608
5	Welker	549	13,236
6	Durgin	709	17,082
7	Applequist	158	3,804
8	Pratt	630	15,198
9	-	36	846
10	-	62	1,476
11	Surveyor	664	16,008
12	Quinn	503	12,108
13	Giacomini	378	9,090
			Total: 160,776

Table 2. Pearson's linear correlation coefficient as a measure of the degree of linear dependence between PC1 and C_{TOT} and indices quantifying cross-shelf velocity and temperature along the 500m isobath (as predicted by the ROMS model) averaged over the upper 100m, and between PC1 and C_{TOT} and the Arctic Oscillation index. No mathematical correction was made for multiple comparisons. Correlations are rounded to two decimal places. Associated p-values are also reported, and correlations with a p-value < 0.1 are indicated with an asterisk.

	PC1		C_{TOT}	
Variable	***r***	***p***	***r***	***p***
East				
Spring Cross Shelf Velocity	-0.31	0.15	-0.09	0.70
Summer Cross Shelf Velocity	-0.33	0.13	-0.20	0.38
Annual Cross Shelf Velocity	-0.62*	<0.01	-0.35	0.11
East Central				
Spring Cross Shelf Velocity	0.06	0.78	0.10	0.65
Summer Cross Shelf Velocity	0.07	0.77	0.13	0.55
Annual Cross Shelf Velocity	0.08	0.74	0.18	0.42
West Central				
Spring Cross Shelf Velocity	-0.06	0.78	0.03	0.88
Summer Cross Shelf Velocity	-0.05	0.81	-0.06	0.79
Annual Cross Shelf Velocity	0.03	0.89	-0.01	0.98
West				
Spring Cross Shelf Velocity	0.21	0.35	0.09	0.69
Summer Cross Shelf Velocity	0.22	0.33	0.24	0.29
Annual Cross Shelf Velocity	0.38	0.08	0.27	0.23
East				
Spring Cross Shelf Temp.	-0.07	0.77	-0.09	0.70
Summer Cross Shelf Temp.	-0.10	0.65	-0.13	0.56
Annual Cross Shelf Temp.	-0.05	0.80	-0.11	0.62
East Central				
Spring Cross Shelf Temp.	-0.13	0.56	-0.19	0.41
Summer Cross Shelf Temp.	-0.18	0.42	-0.18	0.42
Annual Cross Shelf Temp.	-0.09	0.68	-0.15	0.50
West Central				
Spring Cross Shelf Temp.	-0.11	0.64	-0.17	0.46
Summer Cross Shelf Temp.	-0.30	0.18	-0.30	0.17
Annual Cross Shelf Temp.	-0.13	0.56	-0.18	0.42
West				
Spring Cross Shelf Temp.	-0.07	0.75	-0.13	0.56
Summer Cross Shelf Temp.	-0.22	0.32	-0.29	0.19
Annual Cross Shelf Temp.	0.02	0.93	-0.15	0.50
Arctic Oscillation Index				
Jan.-Mar.	0.25	0.26	0.33	0.13
Apr.-Jun.	0.25	0.27	0.17	0.46
Jul.-Sep.	0.64*	<0.01	0.69*	<0.01
Oct.-Dec.	-0.16	0.49	-0.19	0.40

Annual	0.28	0.20	0.30	0.17

Appendix A

Spatially explicitly annual averaged velocity over the GOA for a) 2010 and b) 2018. Velocities were averaged over the upper 100 meters of the water column. The location of the 500m isobath is also shown (dashed line).